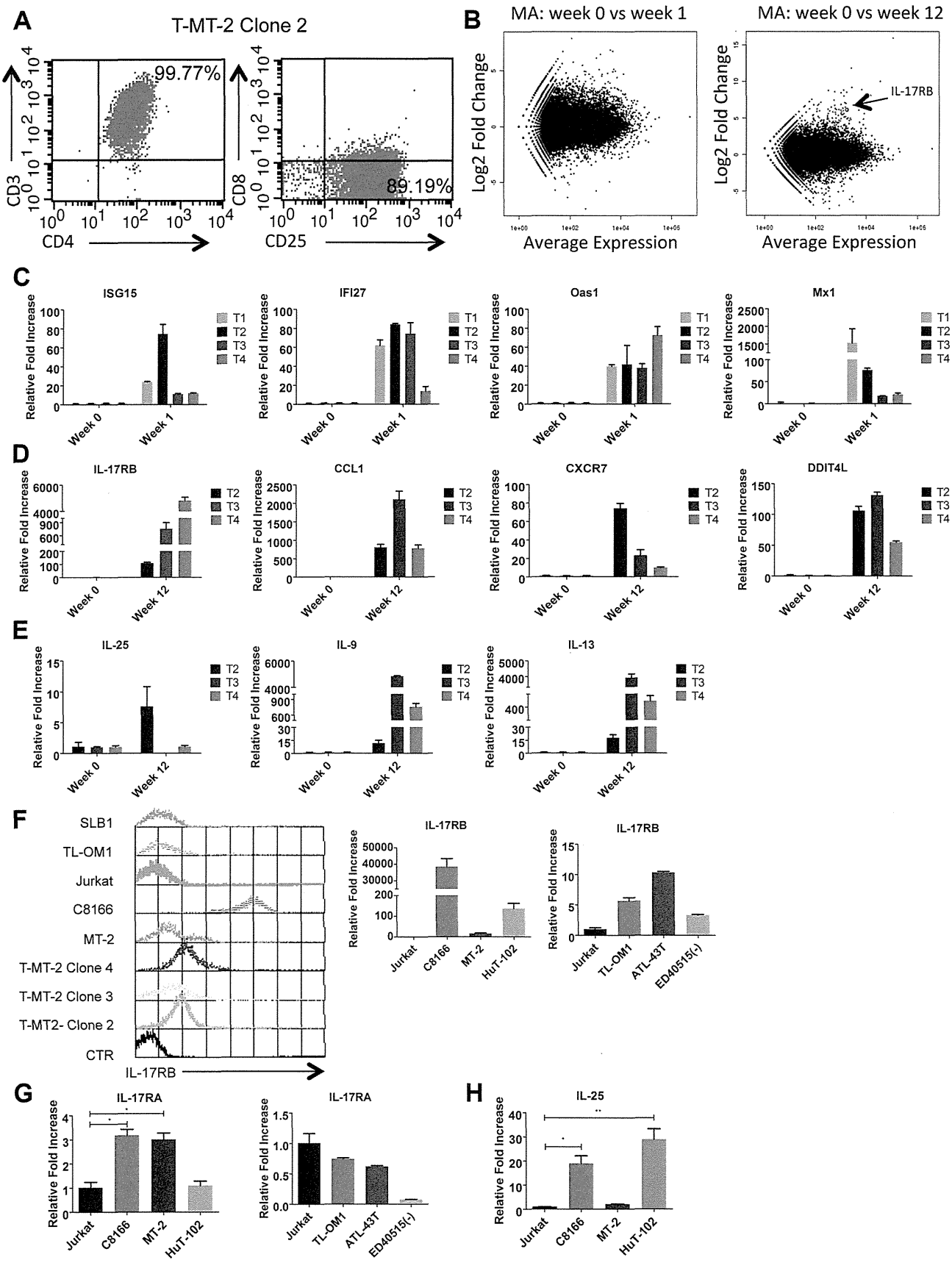
A
T-MT-2 Clone 2
99.77%
89.19%
CD3
CD4
CD8
CD25
B
MA: week 0 vs week 1
MA: week 0 vs week 12
Log2 Fold Change
Average Expression
IL-17RB
C
ISG15
IFI27
Oas1
Mx1
Relative Fold Increase
T1
T2
T3
T4
Week 0
Week 1
D
IL-17RB
CCL1
CXCR7
DDIT4L
Week 12
E
IL-25
IL-9
IL-13
F
SLB1
TL-OM1
Jurkat
C8166
MT-2
T-MT-2 Clone 4
T-MT-2 Clone 3
T-MT2- Clone 2
CTR
IL-17RB
Jurkat
C8166
MT-2
HuT-102
TL-OM1
ATL-43T
ED40515(-)
G
IL-17RA
H
IL-25

Figure 1. IL-17RB is overexpressed in HTLV-1 immortalized T cell clones and transformed cell lines. (**A**) Flow cytometric analysis of CD3/CD4/CD8/CD25 markers with T-MT-2 clone 2. (**B**) Differential gene expression of T cells at week 1 (top) and week 12 (bottom) compared to week 0 (parental T cells) analyzed using RNA-Seq and "DESeq" R package and plotted as an MA plot. DESeq plotMA displays differential expression (log-fold changes) versus expression strength (log average read count). (**C–E**) qRT-PCR of indicated mRNAs in T cell clones. (**F**) Flow cytometric analysis of IL-17RB was performed on the indicated immortalized HTLV-1 immortalized T-cell clones and HTLV-1+ cell lines (top). qRT-PCR of IL-17RB mRNA in HTLV-1+ and ATL cell lines (bottom). (**G, H**) qRT-PCR of IL-17RA and IL-25 mRNAs in HTLV-1+ and ATL cell lines.
doi:10.1371/journal.ppat.1004418.g001

and these results were confirmed by real-time quantitative RT-PCR (qRT-PCR) (Figure 1C and Table S1). Conversely, the HTLV-1-immortalized T cells did not express ISGs, but rather expressed aberrant levels of genes regulating cell growth/cytokines (IL-17RB, IL-5, IL-9, IL-13, CADM1), DNA damage (DDIT4L), cell cycle (CDC14B, CCNA1), metabolism (glycerol kinase 2) and migration/chemokines (CCL1, CXCR7) (Table S2). Also, these immortalized T cells had a distinct genetic signature compared to MT-2 cells (Sequence read archive accession numbers SRS698576 and SRS698477). Notably, many of the aberrantly expressed genes, including IL-17RB, have not previously been linked to transformation by HTLV-1. IL-17RB was one of the most highly induced genes in HTLV-1 immortalized T cells (Figures 1B and S1 and Table S2). IL-17RB mRNA expression was sharply elevated in all 3 independent HTLV-1 immortalized T cell clones as shown by qRT-PCR (Figure 1D). IL-25, the high affinity ligand for IL-17RB, was expressed at variable levels in the three clones (Figure 1E). Aberrant expression of CCL1 (also known as I-309), CXCR7, DDIT4L, IL-9 and IL-13 in HTLV-1-immortalized clones was also confirmed by qRT-PCR (Figure 1D and E). The chemokine CCL1, shown previously to be overexpressed in ATL cells, functions in an anti-apoptotic autocrine loop [40]. Similarly, the chemokine receptor CXCR7 is induced by Tax and regulates the growth and survival of ATL cells [41]. Furthermore, Tax induction of both IL-9 and IL-13 may trigger the autocrine stimulation of HTLV-1 infected cells [42,43]. Taken together, our RNA-Seq studies have confirmed the dysregulation of known targets of HTLV-1 transformation and have also identified genes, such as IL-17RB, not previously demonstrated to be induced by HTLV-1. Next, the cell surface expression of IL-17RB was examined in HTLV-1 transformed cell lines by flow cytometry. IL-17RB was highly expressed in the HTLV-1 immortalized T-cell clones and most HTLV-1-transformed cell lines, but not in Jurkat T cells (Figure 1F). IL-17RB mRNA was also overexpressed in varying degrees in HTLV-1 transformed and ATL cell lines (Figure 1F). Since IL-17RB forms heterodimers with IL-17RA, the expression of IL-17RA was examined in HTLV-1 transformed and ATL cell lines. IL-17RA and IL-25 mRNAs were also upregulated in a subset of HTLV-1 transformed and ATL cell lines (Figure 1G and H).

IL-17RB expression is regulated by Tax and IKK

A previous study reported a role for TGF-β and IL-4 in the upregulation of IL-17RB expression [31]. Since NF-κB is important for the proliferation and survival of HTLV-1 transformed cells, we hypothesized that NF-κB may regulate IL-17RB induction. Thus, the HTLV-1 transformed T-cell lines C8166 and MT-2 were treated with sc-514, a small molecule inhibitor of IKKβ, and qRT-PCR was performed for IL-17RB and the known NF-κB target gene CD25. Treatment with sc-514 significantly diminished the expression of IL-17RB and CD25 mRNAs in these cells (Figure 2A), thus supporting a role for IKKβ and NF-κB in the expression of IL-17RB in HTLV-1 transformed cells. However, sc-514 treatment had no effect on IL-17RB expression in Jurkat cells (Figure 2A). To provide further evidence for a role of IKK in the regulation of IL-17RB, recombinant lentiviruses expressing either control scrambled short hairpin RNA (shRNA) or two distinct shRNAs specific for IKKα or IKKβ were transduced into C8166 cells. Both IKKα and IKKβ shRNAs strongly suppressed their respective mRNAs as shown by qRT-PCR, and these shRNAs significantly inhibited IL-17RB expression (Figure 2B). Therefore, both IKKα and IKKβ regulate IL-17RB expression in C8166 cells.

The HTLV-1 Tax oncoprotein dysregulates the expression of specific cellular genes as part of its oncogenic mechanism [44]. To determine if Tax was involved in the induction of IL-17RB expression we used a Jurkat cell line inducible for Tax expression (Jurkat Tax Tet-On) by doxycycline (Dox) [45]. Jurkat Tax Tet-On cells were treated with Dox for 1, 2 and 3 days and mRNA was harvested for qRT-PCR for IL-17RB. Indeed, induction of Tax strongly upregulated IL-17RB mRNA (Figure 2C). Conversely, shRNA-mediated knockdown of Tax in C8166 cells diminished the expression of IL-17RB mRNA (Figure 2D). Knockdown of Tax also reduced the expression of IL-17RB protein in C8166 cells (Figure 2E). Thus, both gain-of-function and loss-of-function studies support the hypothesis that Tax is the HTLV-1-encoded protein that promotes the aberrant overexpression of IL-17RB.

Two commonly used Tax mutants M22 ($Thr^{130}Leu^{131}$->$Ala^{130}Ser^{131}$) and M47 ($Leu^{319}Leu^{320}$->$Arg^{319}Ser^{320}$) can be used to distinguish NF-κB or CREB-specific functions of Tax [46]. Tax M22 is defective for NF-κB and wild-type for CREB activation, whereas Tax M47 is defective for CREB and wild-type for NF-κB activation. Wild-type Tax, Tax M22 and Tax M47 were cloned into a lentiviral vector and recombinant Tax-expressing lentiviruses were used to transduce Jurkat T cells. Wild-type Tax and Tax M47 strongly upregulated IL-17RB mRNA expression as detected by qRT-PCR, however Tax M22 induction of IL-17RB was significantly diminished (Figure 2F). These data further support the notion that Tax requires NF-κB to induce IL-17RB expression. Interestingly Tax induction of IL-17RB was not observed in 293 cells suggesting that this event may be specific for T cells (Figure 2G). Tax activation of NF-κB was also independent of IL-17RB in 293 cells, since knockdown of IL-17RB in 293 cells had no effect on Tax activation of an NF-κB reporter (Figure 2H). Finally, the expression of IL-25 was not regulated by Tax in T cells, therefore Tax induces the expression of IL-17RB but not its high affinity ligand (Figure 2I).

Tax requires IL-17RB to activate NF-κB in T cells

Since IL-17RB signals to NF-κB, we next asked if Tax required IL-17RB to trigger NF-κB signaling in T cells. Jurkat Tax Tet-On cells were transduced with lentiviruses expressing control or IL-17RB shRNA, yielding ~60–70% knockdown efficiency (Figure 3A). The cells were transiently transfected with NF-κB and HTLV-1 LTR reporters for dual-luciferase assays and also treated with Dox to activate Tax expression. Remarkably, Tax activation of NF-κB, but not the HTLV-1 LTR (which is CREB-mediated), was dependent on IL-17RB (Figure 3A). In agreement with these results, Tax induction of the NF-κB target genes,

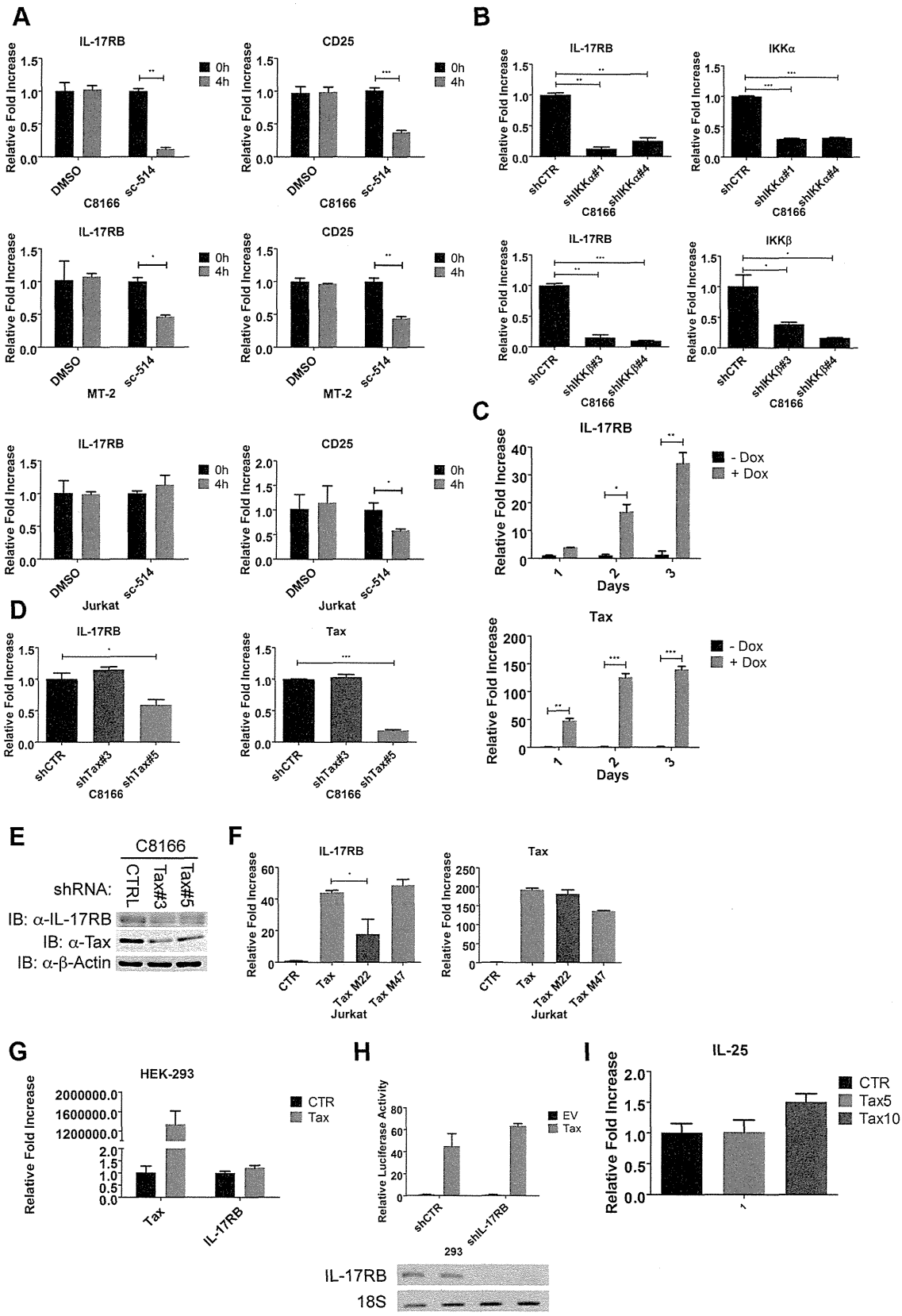

Figure 2. Essential roles for IKK and Tax in the induction of IL-17RB. (**A**) qRT-PCR of IL-17RB and CD25 mRNAs in C8166, MT-2 and Jurkat cells treated with the IKKβ inhibitor sc-514 (10 μM) for 4 h. (**B**) qRT-PCR of IL-17RB, IKKα and IKKβ mRNAs in C8166 cells transduced with lentiviruses expressing control, IKKα or IKKβ shRNAs. (**C**) qRT-PCR of IL-17RB and Tax mRNAs in Jurkat Tax Tet-On cells treated with Dox (1 μg/ml) for the indicated times. (**D**) qRT-PCR of IL-17RB and Tax mRNAs in C8166 cells transduced with lentiviruses expressing control or Tax shRNAs. (**E**) Western blot

of IL-17RB, Tax and β-actin using lysates from C8166 cells transduced with lentiviruses expressing control or the indicated Tax shRNAs. (**F**) qRT-PCR of IL-17RB and Tax mRNAs in Jurkat cells transduced with lentiviruses expressing empty vector (CTR), Tax, Tax M22 or Tax M47. (**G**) qRT-PCR of IL-17RB or Tax mRNAs in 293 cells transduced with lentiviruses expressing empty vector (CTR) or Tax. (**H**) NF-κB luciferase assay with lysates from 293 cells transduced with lentiviruses expressing control (CTR) or IL-17RB shRNA, and then transfected with empty vector (EV) or pCMV4-Tax, together with an NF-κB luciferase reporter and pRL-TK. IL-17RB mRNA and 18S rRNA were detected by RT-PCR (bottom panel). (**I**) qRT-PCR of IL-25 mRNA in Jurkat cells transduced with lentiviruses expressing empty vector (CTR) or Tax at multiplicities of infection (MOIs) of 5 and 10.
doi:10.1371/journal.ppat.1004418.g002

CD25 and cIAP2, was impaired when IL-17RB expression was suppressed with shRNAs (Figure 3B). Therefore, Tax induces IL-17RB expression to establish a positive feedback loop that is critical for Tax-induced NF-κB activation. Also, the requirement of IL-17RB for Tax-mediated NF-κB activation appears to be T-cell specific.

IL-17RB and IL-25 are essential for HTLV-1-induced T-cell immortalization

To determine the role of the IL-17RB pathway in the early events of HTLV-1 transformation of primary human T cells, we conducted an *in vitro* T-cell immortalization assay with irradiated MT-2 cells and PBMCs from normal donors as described earlier. In this co-culture model, expression of both IL-17RB and IL-25 were significantly increased in primary T cells at early times (1–2 weeks) after co-culture with MT-2 cells (Figure 4A). PBMCs were transduced with lentiviruses expressing control shRNA or shRNAs for IL-17RB or IL-25, co-cultured with irradiated MT-2 cells and puromycin was added to select for cells expressing shRNAs. Both IL-17RB and IL-25 were required for immortalization of primary T cells by HTLV-1 since cells expressing these shRNAs ceased to proliferate after 3 weeks of co-culture (Figure 4B). However, as expected PBMCs expressing control shRNA yielded immortalized CD4+ T cells after 8 weeks (Figure 4C). Taken together, these results suggest that both IL-25 and IL-17RB are required for the early events involved in the immortalization of primary T cells by HTLV-1.

IL-17RB is essential for NF-κB signaling and the viability of HTLV-1 transformed T cell lines

Because Tax required IL-17RB for efficient NF-κB activation and NF-κB is critical for the survival of T cells transformed by HTLV-1, we hypothesized that IL-17RB was essential for NF-κB activation and the viability of established HTLV-1 transformed cell lines. To address this notion, recombinant lentiviruses expressing control or IL-17RB shRNAs were transduced into three distinct Tax-expressing HTLV-1 transformed cell lines (C8166, MT-2 and HUT-102). A total of three independent shRNAs to IL-17RB or scrambled control shRNA were expressed in these cell lines and selected with puromycin. Efficient knockdown of IL-17RB was confirmed by qRT-PCR in MT-2 and C8166 cells (Figure 5B). The CellTiter-Glo Luminescent Cell Viability kit was used to quantify cellular ATP levels to determine cell viability and proliferation. Knockdown of IL-17RB significantly reduced the viability and proliferation of HTLV-1 transformed cell lines (Figure 5A). Next, we examined expression of the NF-κB target genes CD25, cIAP2, IRF4 and IL-9 by qRT-PCR. The expression of each of these genes was significantly attenuated upon IL-17RB knockdown in C8166 and MT-2 cells (Figure 5B). Importantly, Tax expression was unaffected by IL-17RB knockdown in these cell lines (Figure 5B).

An NF-κB DNA binding electrophoretic mobility shift assay (EMSA) was next performed with nuclear extracts from C8166, MT-2 and HUT-102 cells expressing control or IL-17RB shRNA. NF-κB DNA binding was completely abrogated upon IL-17RB

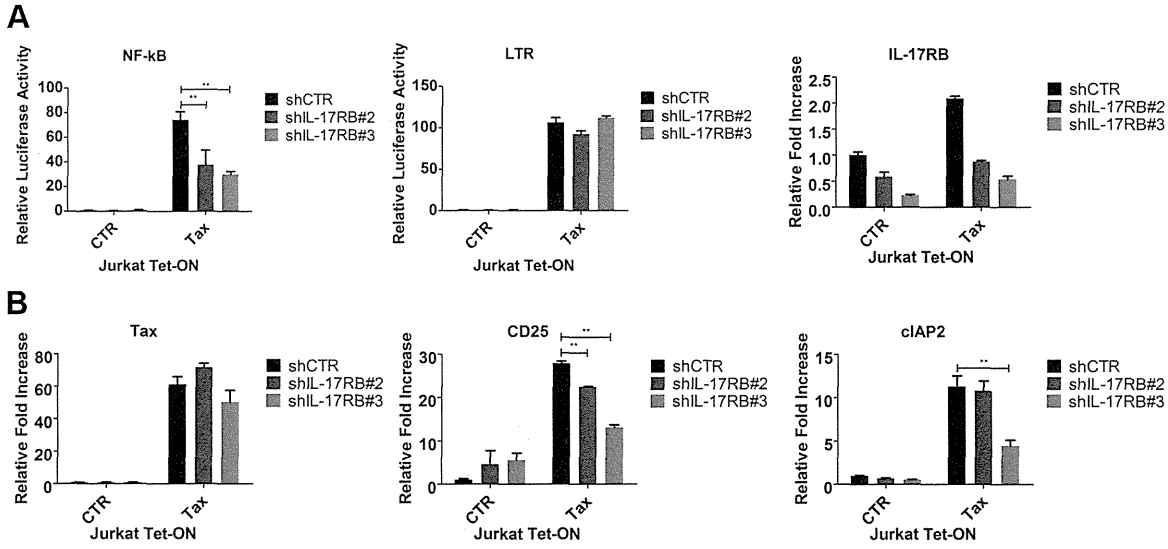

Figure 3. Tax requires IL-17RB for NF-κB activation in T cells. (**A**) NF-κB and HTLV-1 LTR luciferase assays and qRT-PCR of IL-17RB mRNA in Jurkat Tax Tet-On cells transduced with lentiviruses expressing control or IL-17RB shRNA. Cells were also transiently transfected with NF-κB and HTLV-1 LTR luciferase reporters and treated with Dox (1 μg/ml) for 24 h. (**B**) qRT-PCR of Tax, CD25 and cIAP2 mRNAs in Jurkat Tax Tet-On cells from panel (A).
doi:10.1371/journal.ppat.1004418.g003

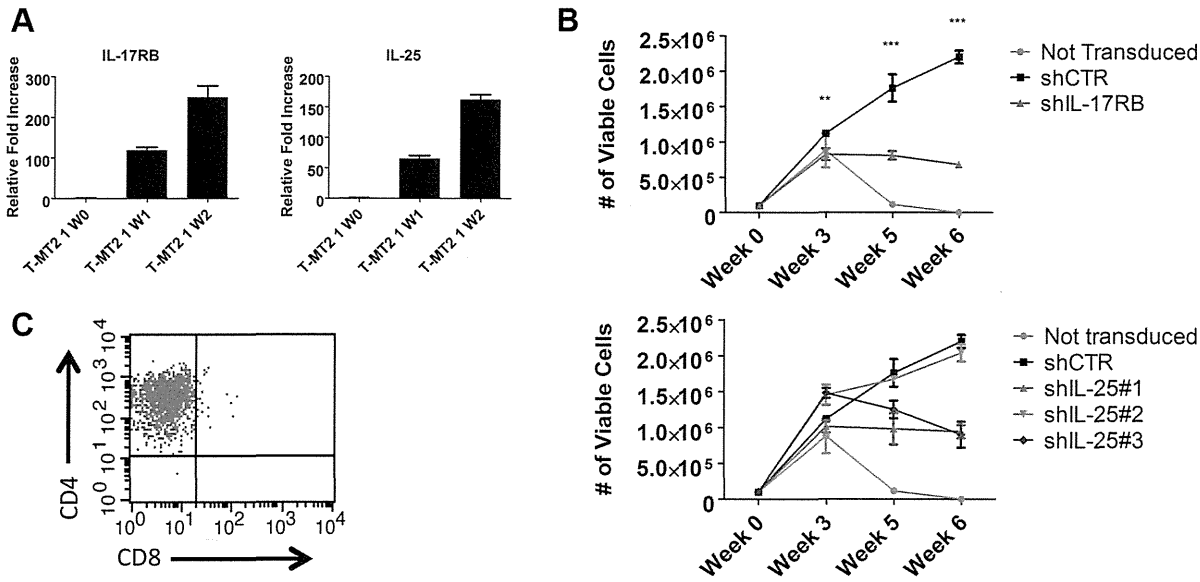

Figure 4. IL-17RB and IL-25 are essential for the HTLV-1-induced immortalization of T cells. (**A**) qRT-PCR of IL-17RB and IL-25 mRNAs in primary T cells co-cultured with lethally irradiated MT-2 cells after 0 (W0), 1 (W1) and 2 (W2) weeks. (**B**) *In vitro* immortalization assay using PBMCs transduced with lentiviruses expressing control (CTR), IL-17RB or IL-25 shRNAs and co-cultured with lethally irradiated MT-2 cells. (**C**) Flow cytometric analysis of CD4 and CD8 markers using immortalized PBMCs expressing control shRNA.
doi:10.1371/journal.ppat.1004418.g004

suppression in C8166 and MT-2 cells, but not HUT-102 likely due to inefficient lentiviral transduction (Figure 5C). IL-25 was also suppressed by shRNAs in MT-2 cells and shRNA#3 was effective in reducing IL-25 expression (Figure 5D). Knockdown of IL-25 with this shRNA also significantly attenuated NF-κB DNA binding and the expression of CD25 (Figure 5C and D). NF-κB signaling can also be monitored with phospho-specific antibodies for IKK and p65 since these proteins are phosphorylated upon activation. Phosphorylation of IKK and p65 was constitutive in C8166, MT-2 and MT-4 cells but reduced upon knockdown of IL-17RB or IL-25 (Figure 5C and E). IκBα protein was increased upon suppression of IL-17RB (Figure 5C), likely reflecting enhanced stability due to a loss of IKK-induced phosphorylation and proteolysis. IL-17RB knockdown also triggered an apoptotic response in HTLV-1 transformed cells as revealed by PARP and caspase 3 cleavage (Figure 5C). The TNFR cell surface receptors CD40 and OX40 activate NF-κB, are strongly induced by Tax and are overexpressed in HTLV-1 transformed cell lines [47,48]. However, knockdown of either CD40 or OX40 had no effect on the proliferation or viability of C8166 cells (Figure 5F). Thus, IL-17RB is a receptor that appears to be uniquely required for NF-κB signaling and the survival of HTLV-1 transformed cells.

IL-9 is a downstream target gene of IL-17RB that controls the proliferation of HTLV-1 transformed T cells

Our earlier results indicated that HTLV-1 immortalized T-cell clones expressed aberrant levels of IL-9 (Figure 1E). A recent study has demonstrated that the IL-17RB pathway controls IL-9 expression in the context of allergic airway inflammation [31]. Furthermore, Tax has been shown to induce IL-9 expression and IL-9 can regulate the proliferation of primary ATL cells [42]. In light of these findings, we hypothesized that IL-9 may represent a key downstream gene of IL-17RB that governs the proliferation of HTLV-1 transformed T cells. First, to determine if IL-17RB regulated a soluble factor that was important for the proliferation of HTLV-1-transformed T cells, C8166 and MT-2 cells were transduced with lentiviruses expressing control or IL-17RB shRNAs and the media was then replaced with conditioned media from the corresponding cells. As expected, suppression of IL-17RB significantly reduced the proliferation of both C8166 and MT-2 cells (Figure 6A). However, the conditioned media rescued the proliferative defects associated with loss of IL-17RB (Figure 6A), suggesting that a soluble factor(s) is sufficient to restore the growth of these cells.

As described above, IL-9 represented an attractive candidate as a pro-proliferative soluble factor in the conditioned media from HTLV-1 transformed T cells. To determine if IL-9 was necessary to restore the proliferation of IL-17RB knockdown cells, we collected conditioned media from cells transduced with control or IL-9 shRNAs for the culture of C8166 cells expressing control or IL-17RB shRNA. Our results revealed that the conditioned media from cells with suppressed IL-9 expression was unable to restore the proliferation of C8166 cells expressing IL-17RB shRNA (Figure 6B). As expected, conditioned media from cells with control shRNA effectively restored C8166 cell growth (Figure 6B). IL-17RB and IL-9 knockdown were confirmed by qRT-PCR (Figure 6B). Next, to determine if IL-9 was sufficient to rescue the growth defect associated with suppressed IL-17RB expression we provided recombinant IL-9 to the media of HTLV-1 transformed cell lines expressing IL-17RB shRNA. The results indicated that provision of IL-9 was sufficient to restore cell proliferation of both C8166 and MT-2 cells (Figure 6C). Therefore, IL-9 is a key cytokine downstream of IL-17RB that governs the proliferation of HTLV-1-transformed T cells.

TRAF6 is required for NF-κB activation in HTLV-1 transformed T cells

IL-17RB can form a heterodimeric receptor complex together with IL-17RA [26], and upon binding to IL-25, the active receptor recruits the Act1 adaptor protein [28]. In addition, the ubiquitin

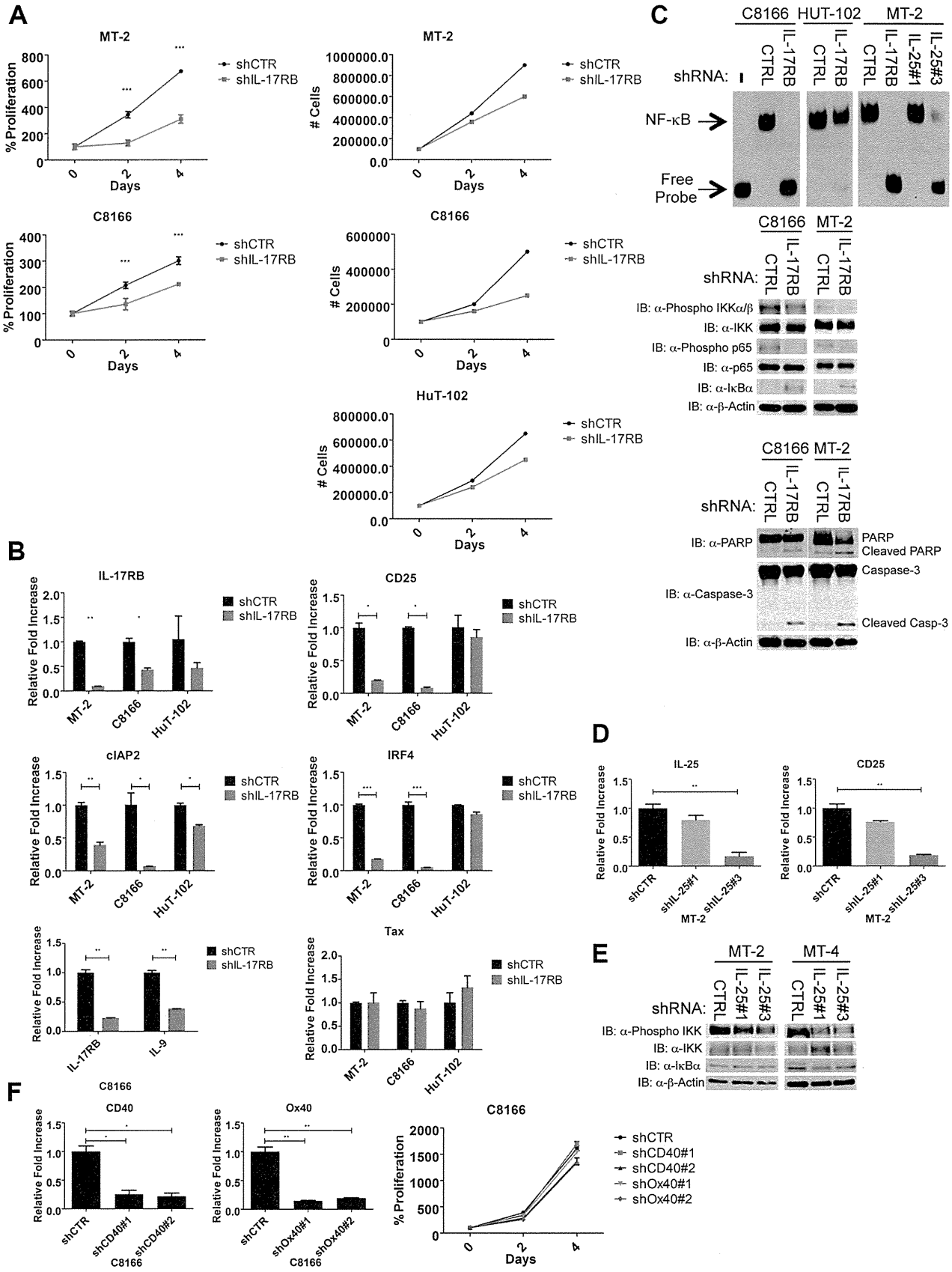

Figure 5. IL-17RB and IL-25 are essential for NF-κB activation and survival of HTLV-1 transformed cells. (**A**) Proliferation/viability assay of MT-2 and C8166 cells transduced with lentiviruses expressing control or IL-17RB shRNA using CellTiter-Glo (left). Cell counts of MT-2, C8166 and HUT-102 cells transduced with control or IL-17RB shRNA. (**B**) qRT-PCR of indicated mRNAs in HTLV-1 transformed cell lines transduced with

lentiviruses expressing control or IL-17RB shRNA. (**C**) NF-κB EMSA using nuclear extracts from MT-2, C8166 and HUT-102 cells transduced with control, IL-17RB or IL-25 shRNAs (left). Western blots were performed with the indicated antibodies using whole-cell lysates from MT-2 and C8166 cells transduced with control, IL-17RB or IL-25 shRNAs (center and right). (**D**) qRT-PCR of CD25 and IL-25 mRNAs in MT-2 cells transduced with lentiviruses expressing control or IL-25 shRNA. (**E**) Western blots were performed with the indicated antibodies using whole cell lysates from MT-2 and MT-4 cells transduced with lentiviruses expressing control or IL-25 shRNAs. (**F**) qRT-PCR of CD40 and OX40 mRNAs in C8166 cells expressing CD40 or OX40 shRNAs (top). Proliferation/viability assay of C8166 cells expressing control, CD40 or OX40 shRNAs.
doi:10.1371/journal.ppat.1004418.g005

ligase TRAF6 can be directly recruited to IL-17RB via a TRAF6 binding motif and plays a critical role in IL-17RB-mediated NF-κB activation and gene expression [30]. Given the vital role of IL-17RB in NF-κB signaling and survival of HTLV-1 transformed T cells, we sought to determine the requirements of the upstream signaling molecules that constitute this pathway. To this end, knockdown experiments were conducted in HTLV-1 transformed cell lines using shRNAs specific for TRAF6, IL-17RA and Act1. Interestingly, knockdown of TRAF6, but not IL-17RA or Act1, attenuated NF-κB activation as determined by western blotting for phosphorylated forms of IKK, p65 and IκBα (Figures 7A, S2C and S3C). Knockdown of TRAF6 also diminished the expression of NF-κB target genes CD25 and cIAP2 as shown by qRT-PCR in HTLV-1 transformed T-cell lines (Figure 7B). Knockdown of IL-17RA, but not Act1, modestly reduced the expression of CD25 and cIAP2 (Figures S2B and S3B). However, the proliferation of HTLV-1 transformed cell lines was strongly dependent on the expression of both IL-17RA and Act1 (Figures S2A and S3A). These results suggest that IL-17RA and Act1 regulate the proliferation of HTLV-1 transformed cells in an NF-κB independent manner. Since IL-17RA regulates chemokine mRNA stability independently of NF-κB [49], this mode of regulation may explain how IL-17RA and Act1 contribute to the proliferation of HTLV-1 transformed T cells.

IL-17RB is essential for NF-κB signaling and survival in a subset of ATL cell lines lacking Tax expression

Thus far our experiments support a model of a Tax-induced IL-17RB-NF-κB feed-forward autocrine loop that is essential for the *in vitro* immortalization of primary T cells by HTLV-1 and the proliferation and survival of established HTLV-1 transformed T cell lines. However, the majority of ATL tumors (~60%) have downregulated or lost Tax expression [19], and these malignant cells have acquired mechanisms to activate NF-κB persistently

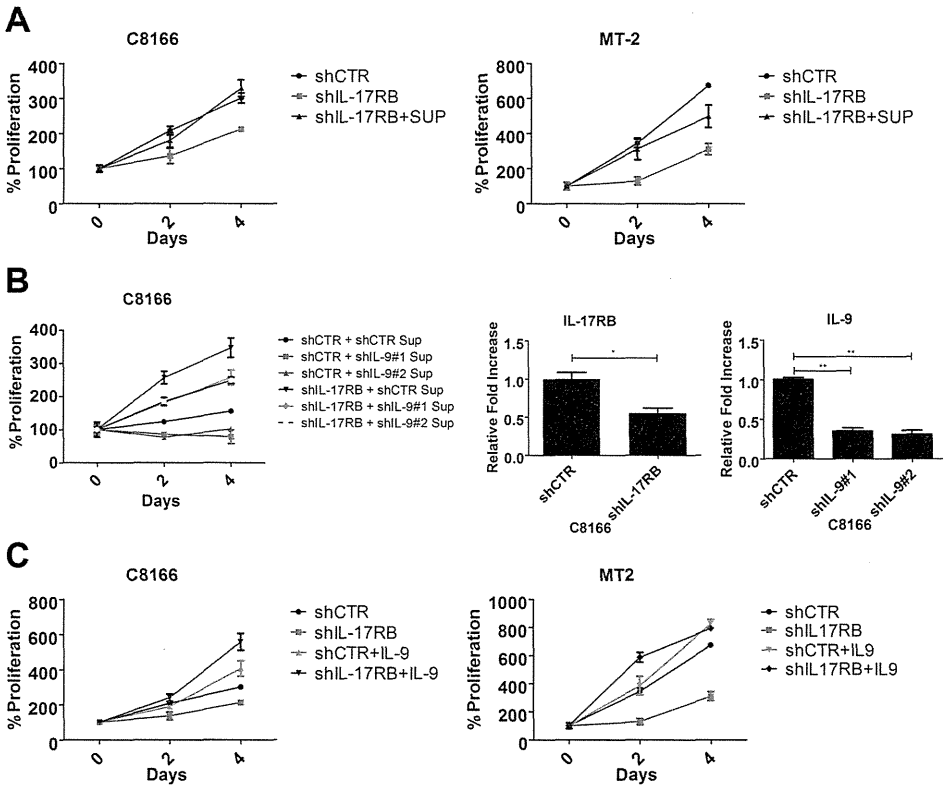

Figure 6. IL-9 is a key target gene downstream of IL-17RB that regulates the proliferation of HTLV-1 transformed cells. (**A**) Proliferation/viability assay of C8166 and MT-2 cells transduced with lentiviruses expressing control or IL-17RB shRNA using CellTiter-Glo. Cells knocked down for IL-17RB were grown in conditioned media (SUP) from the corresponding cell lines. (**B**) Proliferation/viability assay of C8166 cells transduced with lentiviruses expressing control or IL-17RB shRNA. Cells with suppressed IL-17RB expression were grown in conditioned media (Sup) from C8166 expressing control (CTR) or the indicated IL-9 shRNAs (top panel). qRT-PCR of IL-17RB and IL-9 mRNAs in C8166 cells transduced with lentiviruses expressing IL-17RB or IL-9 shRNAs (bottom panel). (**C**) Proliferation/viability assay of C8166 and MT-2 cells transduced with lentiviruses expressing control or IL-17RB shRNA, in the presence or absence of recombinant IL-9 (20 ng/ml) for the indicated times.
doi:10.1371/journal.ppat.1004418.g006

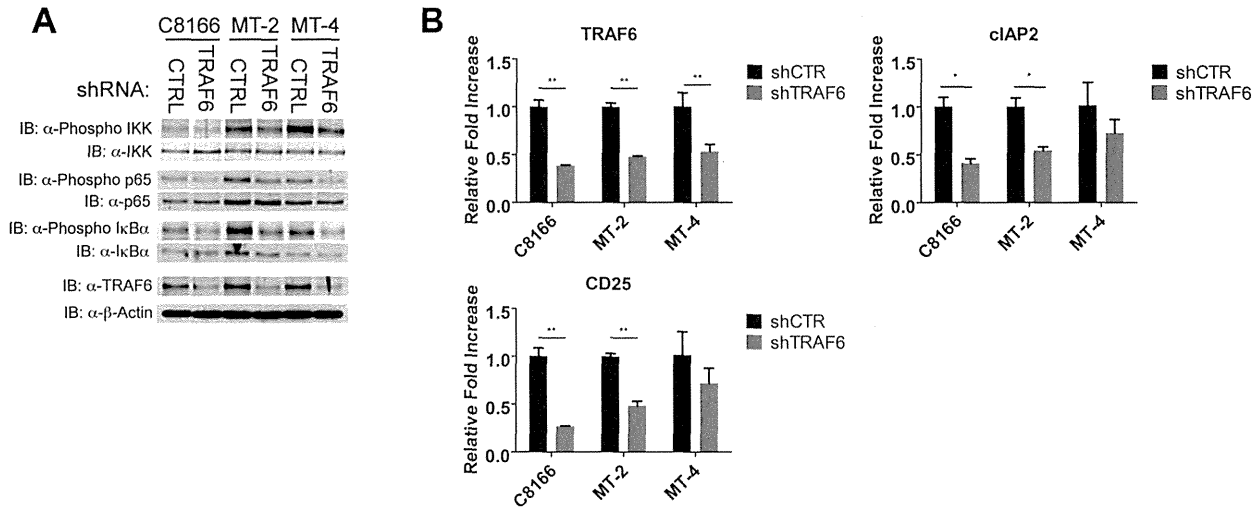

Figure 7. TRAF6 is required for NF-κB activation in HTLV-1 transformed T cells. (**A**) Western blots were performed with the indicated antibodies using whole cell lysates from C8166, MT-2 and MT-4 cells transduced with control or TRAF6 shRNA. (**B**) qRT-PCR of TRAF6, CD25 and cIAP2 mRNAs in C8166, MT-2 and MT-4 cells transduced with lentiviruses expressing control or TRAF6 shRNA.
doi:10.1371/journal.ppat.1004418.g007

despite loss of Tax expression [50]. We next asked if IL-17RB played a role in NF-κB activation in ATL cells lacking Tax expression. Tax-negative ATL cell lines ATL-43T, ED40515(-), TL-OM1 and MT-1 were transduced with control or IL-17RB shRNA lentiviruses. Interestingly, proliferation and viability were significantly diminished in ATL-43T and TL-OM1, but not in ED40515(-), MT-1 and control Jurkat cells (Figure 8A). Knockdown of IL-17RB was efficient in all cell lines except ED40515(-), likely due to poor lentiviral transduction (Figure 8B). Thus, IL-17RB appears to be important for some, but not all Tax-negative ATL cell lines since MT-1 cells proliferated normally despite knockdown of IL-17RB (Figure 8A and B). The NF-κB target genes CD25 and cIAP2 were suppressed in TL-OM1 and ATL-43T cells, but not in the other ATL cell lines (Figure 8B). Phosphorylation of IKK and p65 was also inhibited by IL-17RB knockdown in ATL-43T and TL-OM1 cells (Figure 8C). The loss of NF-κB activation also triggered an apoptotic response as shown by PARP and caspase 3 cleavage (Figure 8C).

We next examined the expression of IL-17RB, IL-17RA, IL-25, IL-17B and Tax in eight primary acute ATL leukemic specimens. IL-17RB expression was significantly overexpressed in 3 out of 8 ATL samples compared to normal control PBMCs (Figure 8D). IL-17RA was modestly elevated in all the ATL samples compared to controls (Figure 8D). However, IL-25 expression was not detected in any of the ATL samples (Figure 8D). Tax mRNA was found in a subset of the samples but did not correlate with IL-17RB expression (Figure 8D), suggesting that ATL cells may regulate IL-17RB expression independently of Tax. Surprisingly, IL-17B was overexpressed in the majority of acute ATL samples (Figure 8E), thus raising the possibility that IL-17B may serve as a ligand for IL-17RB in acute ATL samples.

Discussion

The IL-25-IL-17RB pathway has been linked to allergic airway inflammation and host defense against parasites. Our study has established a novel connection of this pathway to HTLV-1-induced leukemogenesis and also reveal that IL-17RB overexpression can be oncogenic in T cells. Tax promotes the aberrant expression of IL-17RB via NF-κB signaling to establish an IL-17RB-NF-κB feed-forward autocrine loop that drives persistent NF-κB activation in T cells, the natural host cell of HTLV-1. Therefore, Tax has hijacked the IL-17RB-NF-κB signaling axis to sustain high levels of NF-κB and coordinate the induction of a gene program consisting of inflammatory cytokines, chemokines and anti-apoptotic proteins that orchestrates pathogenic T-cell proliferation and survival. Together, these results provide a new framework for how Tax and HTLV-1 persistently activate NF-κB to promote the malignant transformation of T cells.

HTLV-1-induced leukemogenesis is a multi-step process that commences with the IL-2-dependent polyclonal expansion of HTLV-1 infected T cells. The Tax oncoprotein is thought to play critical roles in driving T-cell proliferation and survival in the early events of transformation by HTLV-1. However, at later stages Tax expression is largely dispensable, presumably due to genetic and epigenetic changes that may compensate for the loss of Tax. The HTLV-1-encoded HBZ protein may also exert oncogenic roles in ATL tumors in the absence of Tax expression [51]. Nevertheless, after loss of Tax expression, ATL tumors still exhibit constitutive canonical and noncanonical NF-κB signaling that sustains tumor cell proliferation and survival. However, the mechanisms of Tax-independent NF-κB activation in ATL tumors remain poorly understood. A recent study demonstrated that epigenetic downregulation of the microRNA miR-31 led to overexpression of NIK and activation of noncanonical NF-κB [52]. Our results reveal that IL-17RB drives canonical NF-κB signaling in a subset of ATL cell lines suggesting that the IL-17RB-NF-κB autocrine loop can be maintained in the absence of Tax, most likely by the acquisition of genetic and/or epigenetic changes. Comparative genomic hybridization (CGH) analysis has elucidated specific chromosomal imbalances associated with each of the clinical subtypes of ATL [53]. The highly aggressive acute ATL acquires more frequent chromosomal abnormalities, including characteristic gains at chromosomes 3p, 7q and 14q and losses at chromosomes 6q and 13q [54]. Interestingly, *IL-17RB* is encoded on chromosome 3p21.1, one of the most frequently amplified regions in acute ATL [54]. We found that IL-17RB is significantly overexpressed in leukemic cells from 3/8 ATL patients (38%), comparable to the

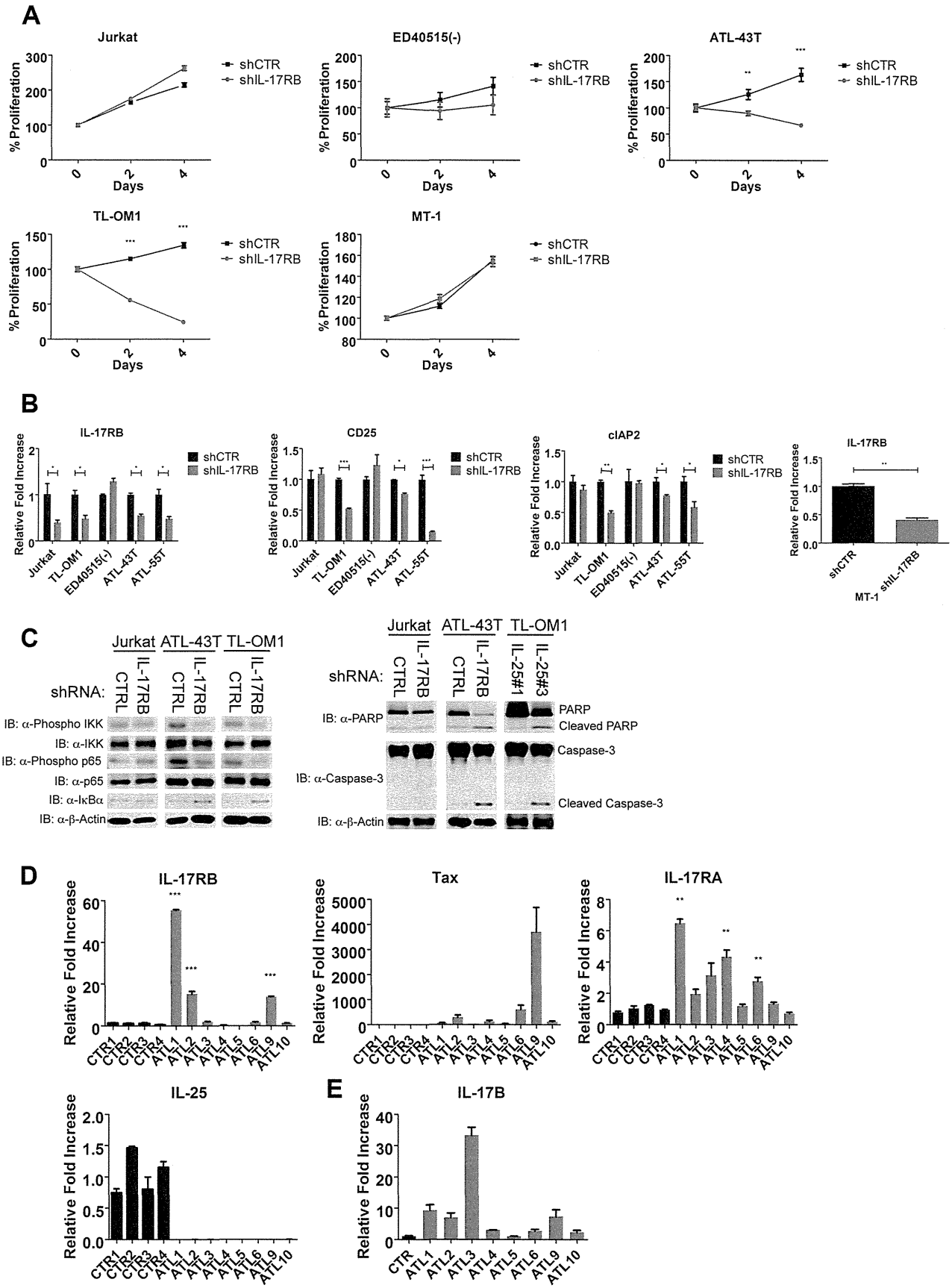
A
Jurkat
ED40515(-)
ATL-43T
TL-OM1
MT-1
% Proliferation
Days
shCTR
shIL-17RB
B
IL-17RB
CD25
cIAP2
Relative Fold Increase
Jurkat
TL-OM1
ED40515(-)
ATL-43T
ATL-55T
shCTR
shIL-17RB
MT-1
C
Jurkat
ATL-43T
TL-OM1
shRNA:
CTRL
IL-17RB
IL-25#1
IL-25#3
IB: α-Phospho IKK
IB: α-IKK
IB: α-Phospho p65
IB: α-p65
IB: α-IκBα
IB: α-β-Actin
IB: α-PARP
PARP
Cleaved PARP
IB: α-Caspase-3
Caspase-3
Cleaved Caspase-3
D
IL-17RB
Tax
IL-17RA
IL-25
CTR1
CTR2
CTR3
CTR4
ATL1
ATL2
ATL3
ATL4
ATL5
ATL6
ATL9
ATL10
E
IL-17B
CTR
ATL1
ATL2
ATL3
ATL4
ATL5
ATL6
ATL9
ATL10

Figure 8. IL-17RB is essential for NF-κB activation and survival in a subset of Tax-negative ATL cell lines. (**A**) Proliferation/viability assay of the indicated cell lines transduced with lentiviruses expressing control or IL-17RB shRNA using CellTiter-Glo. (**B**) qRT-PCR of IL-17RB, CD25 and cIAP2 mRNAs in the indicated cell lines transduced with lentiviruses expressing control or IL-17RB shRNA. (**C**) Western blots were performed using whole cell lysates from the indicated cell lines transduced with control, IL-17RB or IL-25 shRNAs. (**D**) qRT-PCR of IL-17RB, Tax, IL-25 and IL-17RA mRNAs from control PBMCs (normal donors) or primary acute ATL leukemic cells. ATL mRNA expression was compared relative to the average of control mRNA expression. (**E**) qRT-PCR of IL-17B from purified CD4+ T cells (CTR) or primary acute ATL leukemic cells.
doi:10.1371/journal.ppat.1004418.g008

37% of aggressive ATL cases with 3p21 gains [54]. Therefore, IL-17RB overexpression in a subset of acute ATL tumors may potentially regulate the constitutive canonical NF-κB activation in the absence of Tax expression (Figure S4). Nevertheless, additional studies with more ATL patient tumor specimens are warranted to further explore the mechanisms underlying IL-17RB overexpression. It will also be interesting to determine if somatic mutations occur in *IL-17RB* that render the receptor constitutively active in the absence of ligand. Finally, since IL-17B but not IL-25, was expressed by acute ATL leukemic cells (Figure 8), future studies will need to examine if IL-17B plays a role in IL-17RB signaling, NF-κB activation and proliferation of primary ATL cells. IL-25 expression may potentially be suppressed by active mechanisms in ATL since it exerts pro-apoptotic roles in other tumor types [55].

IL-25 serves as the high affinity ligand for IL-17RB. IL-25 favors Th2 immune responses and orchestrates host defense against parasites by inducing the expression of IL-4, IL-5 and IL-13 [56]. IL-25 signals through a heterodimeric receptor containing IL-17RA/IL-17RB, which in turn recruits Act1 and TRAF6 upon IL-25 stimulation to induce NF-κB and MAPK activation that regulate genes important for Th2 immunity, allergic responses and expulsion of helminths. Our results indicate that HTLV-1 transformed cells are critically dependent on the IL-17RB pathway for proliferation, however only IL-17RB and TRAF6 are essential for NF-κB activation. IL-17RB contains a TRAF6 interaction motif in its intracellular domain that propagates downstream NF-κB activation [30]. Furthermore, a previous study has shown that TAK1, a kinase downstream of TRAF6 in the IL-17RB pathway, is also involved in Tax-mediated NF-κB activation [15]. Therefore, IL-17RB may signal through both TRAF6 and TAK1 to activate IKK in HTLV-1 transformed cells. We have recently identified a consensus TRAF6 interaction motif in the C-terminal region of Tax that mediates TRAF6 interaction and activation [57], thus suggesting that Tax may activate TRAF6 to further enhance the Tax-IL-17RB-NF-κB positive feedback loop in T cells. A previous study claimed that TRAF6 was dispensable for Tax-induced NF-κB activation [58], however they used a cell-free assay system using lysates from murine embryonic fibroblasts. Using intact T cells, we found that TRAF6 indeed plays a role in Tax-mediated NF-κB signaling. Our results also indicate that IL-17RB is dispensable for Tax to activate NF-κB in 293 cells, yet is critical for Tax-mediated NF-κB activation in T cells. Therefore, Tax activation of NF-κB appears to be distinct in T cells compared to other cell types and provides a strong rationale for Tax/NF-κB studies to be conducted in T cells.

Our data has provided new insight into the transcriptional regulation of IL-17RB. Little is known regarding how IL-17RB expression is regulated, although a previous study demonstrated that TGF-β and/or IL-4 can induce IL-17RB expression in mouse T cells [31]. We have provided multiple lines of evidence supporting a role for NF-κB in Tax-induced expression of IL-17RB. First, an IKKβ inhibitor greatly reduced the expression of IL-17RB in HTLV-1 transformed T cell lines (Figure 2A). Second, knockdown of IKKα or IKKβ with shRNAs diminished IL-17RB expression in C8166 cells (Figure 2B). Finally, the Tax M22 mutant, defective for NEMO binding and NF-κB activation, was impaired in the induction of IL-17RB (Figure 2F). Taken together, our data support a two-step model of Tax activation of NF-κB in T cells (Figure S4). First, Tax activation of canonical NF-κB commences through direct NEMO/IKK binding and IKK activation. The precise mechanisms remain poorly understood but may involve IKK oligomerization and inhibition of NEMO-associated phosphatase 2A [59,60]. Next, Tax and IKK-induced IL-17RB overexpression (and engagement by IL-25) triggers downstream signaling to TRAF6 and further activates IKK to establish a positive feedback loop resulting in strong and sustained NF-κB signaling. It remains unclear whether NF-κB directly regulates the expression of IL-17RB, although we have identified a putative NF-κB site (GGGAATTTCC) ~3380 base pairs upstream of the human *IL-17RB* transcriptional start site. Future studies will be necessary to identify important regulatory elements in the IL-17RB promoter.

IL-17RB forms heterodimers with IL-17RA, and although IL-17RA does not directly engage IL-25 it appears to be essential for IL-17RB signaling in untransformed cells [26]. Since IL-17RA and Act1 were largely dispensable for NF-κB activation in HTLV-1 transformed cells (Figures S2 and S3), it is plausible that IL-17RA and Act1 regulate the proliferation of these cells by stabilizing chemokine mRNAs [49]. Because IL-17RB is overexpressed to a much greater degree than IL-17RA in HTLV-1 transformed T cells, it is likely that IL-17RB homodimers constitute the most abundant IL-17R complex that signals to NF-κB in these cells. Further studies are needed to examine the stoichiometry of IL-17R complexes and downstream signaling requirements in HTLV-1 transformed cells.

Although IL-25/IL-17RB signaling has been previously linked to the induction of IL-9 and Th2 cytokines [24], our study has identified additional genes regulated by this pathway that contribute to oncogenesis. We found that knockdown of IL-17RB in HTLV-1 transformed cell lines diminished the expression of cytokines (IL-9), cytokine receptors (CD25), anti-apoptotic genes (cIAP2) and transcription factors (IRF4). Elevated expression of IRF4 in ATL tumors was shown to correlate with resistance to antiviral therapy with zidovudine (AZT) and interferon alpha [61]. Furthermore, cIAP2 was identified as a Tax regulated anti-apoptotic gene that was required for the survival of HTLV-1 transformed T cells [62]. IL-9 was also demonstrated to function as a key proliferative factor for ATL cells [42]. Consistently, we found that IL-9 was both necessary and sufficient to restore the cell proliferation of HTLV-1 transformed T cells with IL-17RB knockdown (Figure 6B and C). These data support the notion that IL-9 is an important downstream target gene of IL-17RB that drives the proliferation of HTLV-1 transformed cells. Additional studies will be necessary to identify the full spectrum of genes regulated by IL-17RB in HTLV-1 transformed T cells that support oncogenic proliferation.

Therapeutic blocking antibodies, such as those targeting HER2 and EGFR, have emerged as an important new treatment option in the clinic for carcinomas of the breast, lung and colon [63,64]. IL-17RB is overexpressed in a subset of breast tumors and is

associated with poor prognosis [34]. Treatment with blocking IL-17RB therapeutic antibodies attenuated the tumorigenicity of breast cancer cells [34]. Given that IL-17RB overexpression can promote oncogenic NF-κB signaling in Tax-negative ATL tumors, this receptor may represent an attractive therapeutic target for ATL. IL-17RB may potentially serve as a biomarker to stratify ATL patients that could benefit from IL-17RB inhibition. Preclinical studies with IL-17RB (or potentially IL-17B) monoclonal blocking antibodies in both *in vitro* and *in vivo* ATL models will be required to establish the feasibility of this potential targeted therapy.

Materials and Methods

Ethics statement

Blood from healthy donors was purchased from Biological Specialty Corporation (Colmar, PA). PBMCs were collected from acute ATL patients (n = 8). This study was conducted according to the principles expressed in the Declaration of Helsinki. The study was approved by the Institutional Review Board of Kyoto University (G204). All patients provided written informed consent for the collection of samples and subsequent analysis.

Plasmids, cell lines, recombinant proteins and inhibitors

Human embryonic kidney cells (HEK 293T) and Jurkat T cells were purchased from ATCC. The HTLV-1-transformed cell lines MT-2, HUT-102, C8166 and MT-4 were described previously [65,66]. ED40515(-), MT-1, and TL-OM1 cells are clones of leukemic cells derived from ATL patients, kindly provided by Dr. Michiyuki Maeda (Kyoto University). ATL43T is a Tax-negative ATL cell line that was previously described [67]. Jurkat Tax Tet-On cells were kindly provided by Dr. Warner Greene [45]. 293T cells were cultured in Dulbecco's Modified Eagle's medium (DMEM); Jurkat, MT-2, C8166, MT-4, ATL-43T, HUT-102, ED40515(-), MT-1 and TL-OM1 cells were cultured in RPMI medium. Media was supplemented with fetal bovine serum (FBS; 10%) and penicillin-streptomycin (1×). MISSION shRNAs targeting human IL-17RB, IL-17RA, IL-25, IL-9, Act1, CD40, OX40 and control scrambled shRNA were purchased from Sigma. TRAF6, Tax, IKKα and IKKβ shRNAs were cloned into pYNC352/puro. Target sequences for these shRNAs are listed in Table S3. Tax WT, M22 and M47 were cloned in the pDUET lentiviral vector. Expression vectors encoding κB Luciferase (Luc), pU3R-Luc, pRL-TK (thymidine kinase) have all been described previously [68]. Recombinant human IL-9 was purchased from R&D Systems. The IKKβ inhibitor SC-514 was from EMD Millipore.

Antibodies

The following antibodies were used in this study: anti-hIL-17RB (FAB1207P; R&D Systems), anti-hCD4 (555346; BD Pharmingen), anti-hCD3 (552851; BD Pharmingen), anti-hCD8 (555366; BD Pharmingen), anti-hCD25 (560989; BD Pharmingen), anti-β-actin (AC15; Abcam), anti-IκBα (SC-371; Santa Cruz Biotechnology), anti-phospho-IκBα (14D4; Cell Signaling), anti-p65 (8242S; Cell Signaling), anti-phospho-p65 (3031S; Cell Signaling), anti-IKKβ (2678; Cell Signaling), anti-phospho-IKKα/β (2697S; Cell Signaling), anti-IL-17RB (SC-52925; Santa Cruz Biotechnology), anti-TRAF6 (SC-7221; Santa Cruz Biotechnology), anti-PARP (9542S; Cell Signaling) and anti-caspase-3 (SC-7148; Santa Cruz Biotechnology).

Isolation of PBMCs

Human PBMCs from healthy donors were prepared from lymphocyte enriched human blood with a Ficoll-Hypaque gradient (Pharmacia Biotech). Samples were tested and found to be negative for hepatitis B virus (HBV), hepatitis C virus (HCV) and human immunodeficiency virus 1 (HIV-1). The cells were stimulated for 36 h with phytohemagglutinin (PHA, 2 μg/ml) and then cultured in RPMI medium supplemented with 20% FBS, 2 mM L-glutamine, penicillin-streptomycin, and 25 units/ml of human recombinant IL-2 (Biological Resources Branch, NCI). Under these conditions, PBMCs continuously grew for up to 4 weeks in the presence of exogenous IL-2. CD4+ T cells were isolated from PBMCs by negative selection using MACS MS Columns (Miltenyi Biotec). The purity of the cells was confirmed by flow cytometry and was>95%.

In vitro transformation of T cells with HTLV-I

In vitro transformation of T cells with HTLV-I was performed as previously described [39]. Briefly, PHA-stimulated PBMCs were co-cultured with lethally γ-irradiated (50 Grays (Gy)) HTLV-1 donor cells (MT-2) in IL-2-containing RPMI medium. As expected, the virus-infected T cells became immortalized after about 6 weeks of co-cultivation. These cells proliferated vigorously when exogenous IL-2 was provided, a characteristic of T cells at an early stage of HTLV-1 infection. Under identical culture conditions, the uninfected control T cells or PBMCs typically ceased growth within 4 weeks, and the γ-irradiated MT-2 cells did not proliferate. The HTLV-1-immortalized T cells were maintained in RPMI medium supplemented with IL-2 and used as a bulk population. For shRNA knockdown studies, purified PHA-stimulated PBMCs were first infected with lentiviral particles expressing shRNAs to knockdown the indicated genes and subsequently co-cultured with lethally γ-irradiated (50 Gy) HTLV-1 donor cells (MT-2) in IL-2-containing RPMI medium. Puromycin was added after 3 weeks of co-culture to select for shRNA expressing cells.

RNA-sequencing

Total RNA was prepared from parental primary T cells, HTLV-1-infected cells after 1 week of co-culture, HTLV-1 immortalized T cell clones after 12 weeks of co-culture or MT-2 cells. Dead cells were removed from co-cultured cells after magnetic labeling and separation using the Dead Cell Removal Kit (Miltenyi Biotec). RNA was isolated with RNeasy columns (Qiagen). RNA-Seq and bioinformatics were conducted by the Johns Hopkins Sidney Kimmel Cancer Center next-generation sequencing core. Sequencing analysis was performed by aligning the paired end reads to hg19 using Bioscope. The differential expression analysis was performed using the DEseq R package and the GO enrichment was done with the topGO R package.

Transfections, lentiviral infections and luciferase assays

Jurkat cells were transfected with TransIT-Jurkat (Mirus) according to the manufacturer's instructions. For lentivirus production, HEK293T cells were transfected with a lentiviral vector and gag/pol-encoding plasmids using GenJet (SignaGen) according to the manufacturer's instructions. Virus was harvested after 48 h by centrifugation at 49,000× *g*. Cells were transduced with lentivirus by the spinoculation protocol, cultured for 48 h and then selected with puromycin. For luciferase assays, cells were lysed 24 h after transfection using passive lysis buffer (Promega). Luciferase activity was measured with the dual-luciferase assay system according to the manufacturer's instructions (Promega). Firefly luciferase values were normalized based on the *Renilla* luciferase internal control values. Luciferase values are presented as "fold induction" relative to the shControl (shCTR).

Western blotting and immunoprecipitations

Western blotting was performed essentially as described previously [69]. Whole cell lysates were resolved by SDS-PAGE, transferred to nitrocellulose membranes, blocked in 5% milk or bovine serum albumin (BSA) (for phospho-specific antibodies), incubated with the indicated primary and secondary antibodies, and detected using Western Lightning enhanced chemiluminescence reagent (Perkin Elmer).

Quantitative real time-PCR (qRT-PCR)

Quantitative real-time PCR (qRT-PCR) was performed as described previously [68]. Total RNA was isolated from cells using the RNeasy mini kit (Qiagen). RNA was converted to cDNA using the First Strand cDNA synthesis kit for RT-PCR (avian myeloblastosis virus [AMV]; Roche). Real-time PCR was performed using SYBR Green qPCR (Sigma). Gene expression was normalized to the internal control 18S rRNA. PCR primers are listed in Table S4.

Cell viability and proliferation assays

Cell viability and proliferation assay was determined using the CellTiter-Glo Luminescent Cell Viability Assay (Promega). Cells were cultured in 96-well plates and the ATP content was quantified as an indicator of metabolically active cells.

EMSA

Small-scale nuclear extracts were prepared from cells as described previously [47]. The following sequence was used to generate double-stranded oligonucleotides for electrophoretic mobility shift assays (EMSA): IL-2Rα NF-κB site: 5′-CAACGG-CAGGGGAATCTCCCTCTCCTT. Nonradioactive EMSA was performed using LightShift Chemiluminescent EMSA Kit (Thermo Scientific) according to the manufacturer's instructions.

Statistical analysis

Two-tailed unpaired T test was performed with Prism software. Error bars represent the standard deviation of triplicate samples. The level of significance was defined as: ***$P<0.001$, **$P<0.01$, *$P<0.05$.

Supporting Information

Figure S1 RNA-Seq analysis of IL-17RB in HTLV-1 infected and immortalized T cells. Read coverage and mapping of *IL-17RB* on human genome *Hg19* chromosome 3 using the Integrative Genomics Viewer (Broad Institute). Upper panel represents parental primary T cells (W0), middle panel represents T cells co-cultured with irradiated MT-2 cells for 1 week (W1) and lower panel represents T cells immortalized by HTLV-1 after co-culture for 12 weeks (W12).
(PDF)

Figure S2 IL-17RA regulates the proliferation of HTLV-1 transformed cell lines. (**A**) Proliferation/viability assay of C8166, Jurkat, TL-OM1 and MT-2 cells transduced with lentiviruses expressing control or IL-17RA shRNA using CellTiter-Glo. (**B**) qRT-PCR of indicated mRNAs in C8166 cells transduced with lentiviruses expressing control or IL-17RA shRNA. (**C**). Western blots were performed with the indicated antibodies using whole cell lysates from MT-2 and MT-4 cells transduced with control or IL-17RA shRNAs. Error bars represent the standard deviation of triplicate samples. (***$P<0.001$, **$P<0.01$, *$P<0.05$).
(PDF)

Figure S3 Act1 regulates the proliferation of HTLV-1 transformed cell lines. (**A**) Proliferation/viability assay of C8166 cells transduced with lentiviruses expressing control or Act1 shRNAs using CellTiter-Glo. (**B**) qRT-PCR of CD25 and cIAP2 mRNAs in C8166 cells transduced with lentiviruses expressing control or Act1 shRNAs. (**C**). Western blots were performed with the indicated antibodies using whole cell lysates from MT-2 and MT-4 cells transduced with control or Act1 shRNAs. Error bars represent the standard deviation of triplicate samples. (*$P<0.05$).
(PDF)

Figure S4 Model depicting the role of IL-17RB in HTLV-1-induced leukemogenesis. 1) Tax interacts with IKK and upregulates the expression of IL-17RB. 2) Overexpression of IL-17RB synergizes with Tax to promote a feed-forward NF-κB activation loop. IL-17RA and Act1 do not appear to contribute to NF-κB activation but rather promote cell proliferation, possibly via enhanced chemokine and cytokine mRNA stability. 3) Loss of Tax in malignant ATL cells is associated with genomic instability and chromosome 3p gains in a subset of ATL patients resulting in the potential amplification of IL-17RB and the constitutive activation of NF-κB in the absence of Tax. IL-17B may serve as a ligand for IL-17RB in ATL since IL-25 is not expressed.
(PDF)

Table S1 RNA-Seq results of primary T cells infected with HTLV-1. A list of all transcripts that were upregulated or downregulated by more than 5 log2 fold change ($P\leq0.001$) in primary T cells co-cultured with lethally irradiated MT-2 cells for 1 week.
(XLSM)

Table S2 RNA-Seq results of primary T cells immortalized with HTLV-1. A list of all transcripts that were upregulated or downregulated by more than 5 log2 fold change ($P\leq0.001$) in primary T cells immortalized with HTLV-1 (primary T cells were co-cultured with lethally irradiated MT-2 cells for 12 weeks).
(XLSM)

Table S3 Oligonucleotide sequences for shRNAs.
(PDF)

Table S4 Primer sequences for qRT-PCR.
(PDF)

Acknowledgments

We thank Dr. Warner Greene for Jurkat Tax Tet-On cells and Dr. Michiyuki Maeda for TL-OM1 and ED40515(-) ATL cell lines. We also acknowledge Dr. Young Bong Choi for generating TRAF6, Tax and IKK shRNA lentiviruses.

Author Contributions

Conceived and designed the experiments: AL EWH. Performed the experiments: AL. Analyzed the data: AL EWH. Contributed reagents/materials/analysis tools: MM. Wrote the paper: AL EWH.

References

1. Gallo RC (2011) Research and discovery of the first human cancer virus, HTLV-1. Best Pract Res Clin Haematol 24: 559–565.
2. Yasunaga J, Matsuoka M (2011) Molecular mechanisms of HTLV-1 infection and pathogenesis. Int J Hematol 94: 435–442.

3. Izumo S, Umehara F, Osame M (2000) HTLV-I-associated myelopathy. Neuropathology 20 Suppl: S65–68.
4. Iwanaga M, Watanabe T, Yamaguchi K (2012) Adult T-cell leukemia: a review of epidemiological evidence. Front Microbiol 3: 322.
5. Matsuoka M, Jeang KT (2007) Human T-cell leukaemia virus type 1 (HTLV-1) infectivity and cellular transformation. Nat Rev Cancer 7: 270–280.
6. Sun SC, Yamaoka S (2005) Activation of NF-kappaB by HTLV-I and implications for cell transformation. Oncogene 24: 5952–5964.
7. Hayden MS, Ghosh S (2008) Shared principles in NF-kappaB signaling. Cell 132: 344–362.
8. Sun SC, Ganchi PA, Ballard DW, Greene WC (1993) NF-kappa B controls expression of inhibitor I kappa B alpha: evidence for an inducible autoregulatory pathway. Science 259: 1912–1915.
9. Karin M, Ben-Neriah Y (2000) Phosphorylation meets ubiquitination: the control of NF-[kappa]B activity. Annu Rev Immunol 18: 621–663.
10. DiDonato JA, Hayakawa M, Rothwarf DM, Zandi E, Karin M (1997) A cytokine-responsive IkappaB kinase that activates the transcription factor NF-kappaB. Nature 388: 548–554.
11. Harhaj EW, Sun SC (1999) IKKgamma serves as a docking subunit of the IkappaB kinase (IKK) and mediates interaction of IKK with the human T-cell leukemia virus Tax protein. J Biol Chem 274: 22911–22914.
12. Harhaj EW, Good L, Xiao G, Uhlik M, Cvijic ME, et al. (2000) Somatic mutagenesis studies of NF-kappa B signaling in human T cells: evidence for an essential role of IKK gamma in NF-kappa B activation by T-cell costimulatory signals and HTLV-I Tax protein. Oncogene 19: 1448–1456.
13. Chu ZL, Shin YA, Yang JM, DiDonato JA, Ballard DW (1999) IKKgamma mediates the interaction of cellular IkappaB kinases with the tax transforming protein of human T cell leukemia virus type 1. J Biol Chem 274: 15297–15300.
14. Xiao G, Cvijic ME, Fong A, Harhaj EW, Uhlik MT, et al. (2001) Retroviral oncoprotein Tax induces processing of NF-kappaB2/p100 in T cells: evidence for the involvement of IKKalpha. EMBO J 20: 6805–6815.
15. Wu X, Sun SC (2007) Retroviral oncoprotein Tax deregulates NF-kappaB by activating Tak1 and mediating the physical association of Tak1-IKK. EMBO Rep 8: 510–515.
16. Geleziunas R, Ferrell S, Lin X, Mu Y, Cunningham ET, Jr., et al. (1998) Human T-cell leukemia virus type 1 Tax induction of NF-kappaB involves activation of the IkappaB kinase alpha (IKKalpha) and IKKbeta cellular kinases. Mol Cell Biol 18: 5157–5165.
17. Robek MD, Ratner L (1999) Immortalization of CD4(+) and CD8(+) T lymphocytes by human T-cell leukemia virus type 1 Tax mutants expressed in a functional molecular clone. J Virol 73: 4856–4865.
18. Mori N, Fujii M, Ikeda S, Yamada Y, Tomonaga M, et al. (1999) Constitutive activation of NF-kappaB in primary adult T-cell leukemia cells. Blood 93: 2360–2368.
19. Takeda S, Maeda M, Morikawa S, Taniguchi Y, Yasunaga J, et al. (2004) Genetic and epigenetic inactivation of tax gene in adult T-cell leukemia cells. Int J Cancer 109: 559–567.
20. Gu C, Wu L, Li X (2013) IL-17 family: cytokines, receptors and signaling. Cytokine 64: 477–485.
21. Gaffen SL (2009) Structure and signalling in the IL-17 receptor family. Nat Rev Immunol 9: 556–567.
22. Pan G, French D, Mao W, Maruoka M, Risser P, et al. (2001) Forced expression of murine IL-17E induces growth retardation, jaundice, a Th2-biased response, and multiorgan inflammation in mice. J Immunol 167: 6559–6567.
23. Petersen BC, Lukacs NW (2012) IL-17A and IL-25: therapeutic targets for allergic and exacerbated asthmatic disease. Future Med Chem 4: 833–836.
24. Angkasekwinai P, Park H, Wang YH, Wang YH, Chang SH, et al. (2007) Interleukin 25 promotes the initiation of proallergic type 2 responses. J Exp Med 204: 1509–1517.
25. Ikeda K, Nakajima H, Suzuki K, Kagami S, Hirose K, et al. (2003) Mast cells produce interleukin-25 upon Fc epsilon RI-mediated activation. Blood 101: 3594–3596.
26. Rickel EA, Siegel LA, Yoon BR, Rottman JB, Kugler DG, et al. (2008) Identification of functional roles for both IL-17RB and IL-17RA in mediating IL-25-induced activities. J Immunol 181: 4299–4310.
27. Lee J, Ho WH, Maruoka M, Corpuz RT, Baldwin DT, et al. (2001) IL-17E, a novel proinflammatory ligand for the IL-17 receptor homolog IL-17Rh1. J Biol Chem 276: 1660–1664.
28. Claudio E, Sonder SU, Saret S, Carvalho G, Ramalingam TR, et al. (2009) The adaptor protein CIKS/Act1 is essential for IL-25-mediated allergic airway inflammation. J Immunol 182: 1617–1630.
29. Swaidani S, Bulek K, Kang Z, Liu C, Lu Y, et al. (2009) The critical role of epithelial-derived Act1 in IL-17- and IL-25-mediated pulmonary inflammation. J Immunol 182: 1631–1640.
30. Maezawa Y, Nakajima H, Suzuki K, Tamachi T, Ikeda K, et al. (2006) Involvement of TNF receptor-associated factor 6 in IL-25 receptor signaling. J Immunol 176: 1013–1018.
31. Angkasekwinai P, Chang SH, Thapa M, Watarai H, Dong C (2010) Regulation of IL-9 expression by IL-25 signaling. Nat Immunol 11: 250–256.
32. Chang SH, Dong C (2011) Signaling of interleukin-17 family cytokines in immunity and inflammation. Cell Signal 23: 1069–1075.
33. Tian E, Sawyer JR, Largaespada DA, Jenkins NA, Copeland NG, et al. (2000) Evi27 encodes a novel membrane protein with homology to the IL17 receptor. Oncogene 19: 2098–2109.
34. Huang CK, Yang CY, Jeng YM, Chen CL, Wu HH, et al. (2014) Autocrine/paracrine mechanism of interleukin-17B receptor promotes breast tumorigenesis through NF-kappaB-mediated antiapoptotic pathway. Oncogene 33: 2968–2977.
35. Harhaj EW, Good L, Xiao G, Sun SC (1999) Gene expression profiles in HTLV-I-immortalized T cells: deregulated expression of genes involved in apoptosis regulation. Oncogene 18: 1341–1349.
36. de La Fuente C, Deng L, Santiago F, Arce L, Wang L, et al. (2000) Gene expression array of HTLV type 1-infected T cells: Up-regulation of transcription factors and cell cycle genes. AIDS Res Hum Retroviruses 16: 1695–1700.
37. Pise-Masison CA, Radonovich M, Dohoney K, Morris JC, O'Mahony D, et al. (2009) Gene expression profiling of ATL patients: compilation of disease-related genes and evidence for TCF4 involvement in BIRC5 gene expression and cell viability. Blood 113: 4016–4026.
38. Wang Z, Gerstein M, Snyder M (2009) RNA-Seq: a revolutionary tool for transcriptomics. Nat Rev Genet 10: 57–63.
39. Persaud D, Munoz JL, Tarsis SL, Parks ES, Parks WP (1995) Time course and cytokine dependence of human T-cell lymphotropic virus type 1 T-lymphocyte transformation as revealed by a microtiter infectivity assay. J Virol 69: 6297–6303.
40. Ruckes T, Saul D, Van Snick J, Hermine O, Grassmann R (2001) Autocrine antiapoptotic stimulation of cultured adult T-cell leukemia cells by overexpression of the chemokine I-309. Blood 98: 1150–1159.
41. Jin Z, Nagakubo D, Shirakawa AK, Nakayama T, Shigeta A, et al. (2009) CXCR7 is inducible by HTLV-1 Tax and promotes growth and survival of HTLV-1-infected T cells. Int J Cancer 125: 2229–2235.
42. Chen J, Petrus M, Bryant BR, Phuc Nguyen V, Stamer M, et al. (2008) Induction of the IL-9 gene by HTLV-I Tax stimulates the spontaneous proliferation of primary adult T-cell leukemia cells by a paracrine mechanism. Blood 111: 5163–5172.
43. Chung HK, Young HA, Goon PK, Heidecker G, Princler GL, et al. (2003) Activation of interleukin-13 expression in T cells from HTLV-1-infected individuals and in chronically infected cell lines. Blood 102: 4130–4136.
44. Ng PW, Iha H, Iwanaga Y, Bittner M, Chen Y, et al. (2001) Genome-wide expression changes induced by HTLV-1 Tax: evidence for MLK-3 mixed lineage kinase involvement in Tax-mediated NF-kappaB activation. Oncogene 20: 4484–4496.
45. Kwon H, Ogle L, Benitez B, Bohuslav J, Montano M, et al. (2005) Lethal cutaneous disease in transgenic mice conditionally expressing type I human T cell leukemia virus Tax. J Biol Chem 280: 35713–35722.
46. Smith MR, Greene WC (1990) Identification of HTLV-I tax trans-activator mutants exhibiting novel transcriptional phenotypes. Genes Dev 4: 1875–1885.
47. Harhaj EW, Harhaj NS, Grant C, Mostoller K, Alefantis T, et al. (2005) Human T cell leukemia virus type I Tax activates CD40 gene expression via the NF-kappa B pathway. Virology 333: 145–158.
48. Saito M, Tanaka R, Arishima S, Matsuzaki T, Ishihara S, et al. (2013) Increased expression of OX40 is associated with progressive disease in patients with HTLV-1-associated myelopathy/tropical spastic paraparesis. Retrovirology 10: 51.
49. Sun D, Novotny M, Bulek K, Liu C, Li X, et al. (2011) Treatment with IL-17 prolongs the half-life of chemokine CXCL1 mRNA via the adaptor TRAF5 and the splicing-regulatory factor SF2 (ASF). Nat Immunol 12: 853–860.
50. Hironaka N, Mochida K, Mori N, Maeda M, Yamamoto N, et al. (2004) Tax-independent constitutive IkappaB kinase activation in adult T-cell leukemia cells. Neoplasia 6: 266–278.
51. Zhao T, Matsuoka M (2012) HBZ and its roles in HTLV-1 oncogenesis. Front Microbiol 3: 247.
52. Yamagishi M, Nakano K, Miyake A, Yamochi T, Kagami Y, et al. (2012) Polycomb-mediated loss of miR-31 activates NIK-dependent NF-kappaB pathway in adult T cell leukemia and other cancers. Cancer Cell 21: 121–135.
53. Oshiro A, Tagawa H, Ohshima K, Karube K, Uike N, et al. (2006) Identification of subtype-specific genomic alterations in aggressive adult T-cell leukemia/lymphoma. Blood 107: 4500–4507.
54. Tsukasaki K, Krebs J, Nagai K, Tomonaga M, Koeffler HP, et al. (2001) Comparative genomic hybridization analysis in adult T-cell leukemia/lymphoma: correlation with clinical course. Blood 97: 3875–3881.
55. Furuta S, Jeng YM, Zhou L, Huang L, Kuhn I, et al. (2011) IL-25 causes apoptosis of IL-25R-expressing breast cancer cells without toxicity to nonmalignant cells. Sci Transl Med 3: 78ra31.
56. Fort MM, Cheung J, Yen D, Li J, Zurawski SM, et al. (2001) IL-25 induces IL-4, IL-5, and IL-13 and Th2-associated pathologies in vivo. Immunity 15: 985–995.
57. Choi YB, Harhaj EW (2014) HTLV-1 Tax stabilizes MCL-1 via TRAF6-dependent K63-linked polyubiquitination to promote cell survival and transformation. PLoS Pathog: [In Press].
58. Shibata Y, Tanaka Y, Gohda J, Inoue J (2011) Activation of the IkappaB kinase complex by HTLV-1 Tax requires cytosolic factors involved in Tax-induced polyubiquitination. J Biochem 150: 679–686.
59. Huang GJ, Zhang ZQ, Jin DY (2002) Stimulation of IKK-gamma oligomerization by the human T-cell leukemia virus oncoprotein Tax. FEBS Lett 531: 494–498.
60. Fu DX, Kuo YL, Liu BY, Jeang KT, Giam CZ (2003) Human T-lymphotropic virus type I tax activates I-kappa B kinase by inhibiting I-kappa B kinase-associated serine/threonine protein phosphatase 2A. J Biol Chem 278: 1487–1493.

61. Ramos JC, Ruiz P, Jr., Ratner L, Reis IM, Brites C, et al. (2007) IRF-4 and c-Rel expression in antiviral-resistant adult T-cell leukemia/lymphoma. Blood 109: 3060–3068.
62. Waldele K, Silbermann K, Schneider G, Ruckes T, Cullen BR, et al. (2006) Requirement of the human T-cell leukemia virus (HTLV-1) tax-stimulated HIAP-1 gene for the survival of transformed lymphocytes. Blood 107: 4491–4499.
63. Slamon DJ, Leyland-Jones B, Shak S, Fuchs H, Paton V, et al. (2001) Use of chemotherapy plus a monoclonal antibody against HER2 for metastatic breast cancer that overexpresses HER2. N Engl J Med 344: 783–792.
64. Ciardiello F, Tortora G (2001) A novel approach in the treatment of cancer: targeting the epidermal growth factor receptor. Clin Cancer Res 7: 2958–2970.
65. Charoenthongtrakul S, Zhou Q, Shembade N, Harhaj NS, Harhaj EW (2011) Human T cell leukemia virus type 1 Tax inhibits innate antiviral signaling via NF-kappaB-dependent induction of SOCS1. J Virol 85: 6955–6962.
66. Harhaj NS, Janic B, Ramos JC, Harrington WJ, Jr., Harhaj EW (2007) Deregulated expression of CD40 ligand in HTLV-I infection: distinct mechanisms of downregulation in HTLV-I-transformed cell lines and ATL patients. Virology 362: 99–108.
67. Hagiya K, Yasunaga J, Satou Y, Ohshima K, Matsuoka M (2011) ATF3, an HTLV-1 bZip factor binding protein, promotes proliferation of adult T-cell leukemia cells. Retrovirology 8: 19.
68. Lavorgna A, Harhaj EW (2012) An RNA interference screen identifies the Deubiquitinase STAMBPL1 as a critical regulator of human T-cell leukemia virus type 1 tax nuclear export and NF-kappaB activation. J Virol 86: 3357–3369.
69. Shembade N, Ma A, Harhaj EW (2010) Inhibition of NF-kappaB signaling by A20 through disruption of ubiquitin enzyme complexes. Science 327: 1135–1139.

Regular Article

LYMPHOID NEOPLASIA

The role of HTLV-1 clonality, proviral structure, and genomic integration site in adult T-cell leukemia/lymphoma

Lucy B. Cook,[1] Anat Melamed,[1] Heather Niederer,[1] Mikel Valganon,[2,3] Daniel Laydon,[1] Letizia Foroni,[2,3] Graham P. Taylor,[4] Masao Matsuoka,[5] and Charles R. M. Bangham[1]

[1]Section of Immunology, Wright-Fleming Institute, Imperial College, London, United Kingdom; [2]Imperial Molecular Pathology Laboratory, Imperial College Healthcare NHS Trust and Academic Health Sciences Centre, Hammersmith Hospital, London, United Kingdom; [3]Centre for Haematology, Faculty of Medicine, Imperial College, Hammersmith Hospital, London, United Kingdom; [4]Section of Virology, Wright-Fleming Institute, Imperial College, London, United Kingdom; and [5]Institute for Viral Research, Kyoto University, Kyoto, Japan

Key Points

- Adult T-cell leukemia (ATL) does not, as previously believed, result from the oligoclonal proliferation caused by HTLV-1 infection.
- In both ATL patients and those with nonmalignant infection, the HTLV-1 provirus preferentially survives in vivo in acrocentric chromosomes.

Adult T-cell leukemia/lymphoma (ATL) occurs in ~5% of human T-lymphotropic virus type 1 (HTLV-1)–infected individuals and is conventionally thought to be a monoclonal disease in which a single HTLV-1$^+$ T-cell clone progressively outcompetes others and undergoes malignant transformation. Here, using a sensitive high-throughput method, we quantified clonality in 197 ATL cases, identified genomic characteristics of the proviral integration sites in malignant and nonmalignant clones, and investigated the proviral features (genomic structure and 5′ long terminal repeat methylation) that determine its capacity to express the HTLV-1 oncoprotein Tax. Of the dominant, presumed malignant clones, 91% contained a single provirus. The genomic characteristics of the integration sites in the ATL clones resembled those of the frequent low-abundance clones (present in both ATL cases and carriers) and not those of the intermediate-abundance clones observed in 24% of ATL cases, suggesting that oligoclonal proliferation per se does not cause malignant transformation. Gene ontology analysis revealed an association in 6% of cases between ATL and integration near host genes in 3 functional categories, including genes previously implicated in hematologic malignancies. In all cases of HTLV-1 infection, regardless of ATL, there was evidence of preferential survival of the provirus in vivo in acrocentric chromosomes (13, 14, 15, 21, and 22). (*Blood.* 2014;123(25):3925-3931)

Introduction

Human T-lymphotropic virus type 1 (HTLV-1) causes adult T-cell leukemia/lymphoma (ATL) in approximately 5% of HTLV-1–infected individuals. A further ~5% of carriers develop an aggressive myelopathy known as HTLV-1–associated myelopathy (HAM) or other inflammatory diseases such as polymyositis. It remains uncertain why a minority develop aggressive clinical disease, typically decades following asymptomatic infection, whereas most infected individuals remain lifelong healthy carriers. The Shimoyama classification of ATL[1] contains 4 subtypes: acute, lymphoma, chronic, and smoldering. These subtypes differ in the response to treatment and overall survival, but little is known about either viral or host molecular determinants of disease. Several host cytogenetic or molecular defects have been described, but no recurrent genetic lesions have been identified.

The major predictor of clinical disease is the proviral load (PVL), the percentage of HTLV-1–infected peripheral blood mononuclear cells (PBMCs). The PVL remains relatively constant over years within an individual, rising slowly over decades.[2] However, the PVL varies widely between patients, ranging from <0.001% PBMCs to >100% (ie, >100 copies per 100 PBMCs); the risk of disease rises in carriers with a PVL >4% in Japan[3] and in those with a PVL >10% in the United Kingdom.[4] Nonetheless, there is overlap in the range of PVL seen between patients with disease and those that remain lifelong asymptomatic carriers, making individual patient prognosis difficult.

HTLV-1 appears to persist in chronic infection chiefly by mitotic proliferation of infected CD4$^+$ T cells, although the ratio of this mitotic spread to de novo infection[5] has not been rigorously estimated. Each clone of HTLV-1–infected cells can be identified by its particular integration site of the HTLV-1 provirus in the host genome[6]; the daughter cells of each clone share the same genomic integration site, and the frequency of these cells defines the abundance of a given clone. A majority of naturally infected cells in nonmalignant infection contain a single integrated provirus.[7]

ATL is characterized by monoclonal proliferation of CD4$^+$CD25$^+$ tumor cells. For many years, it has been believed that ATL arises following a steady progression from polyclonal infection of CD4$^+$ T cells to an oligoclonal expansion and, many years later, following a series of undefined genetic or epigenetic events, malignant transformation of a previously abundant clone to a monoclonal tumor. However, there are indications that HTLV-1 clonality in ATL may be

Submitted February 1, 2014; accepted April 3, 2014. Prepublished online as *Blood* First Edition paper, April 15, 2014; DOI 10.1182/blood-2014-02-553602.

A.M., H.N., and M.V. contributed equally to this study.

The online version of this article contains a data supplement.

The publication costs of this article were defrayed in part by page charge payment. Therefore, and solely to indicate this fact, this article is hereby marked "advertisement" in accordance with 18 USC section 1734.

more complex. One or more abnormally abundant clones may underlie the largest, putatively malignant clone,[6] and there are reports of "clonal succession" in which a malignant clone spontaneously regresses and an independent clone proliferates in its place.[8]

HTLV-1 expresses a transcriptional transactivator protein, Tax, which activates transcription of the HTLV-1 provirus and of many host genes[9]. Because Tax can immortalize rodent cells in vitro and Tax transgenic mice develop tumors, it has been widely accepted that Tax plays a role in leukemogenesis. This hypothesis is supported by the observations that Tax promotes DNA replication and cell-cycle progression, causes structural damage to host DNA, and inhibits DNA repair and cell-cycle checkpoints.[9] Tax expression is lost in ~40% of ATL cases, probably under selection from the strong anti-Tax cytotoxic T-lymphocyte (CTL) response,[10] but the relation between Tax expression and ATL subtype and progression is unclear. There is also increasing evidence that another HTLV-1 gene, *HBZ*, plays a critical part in leukemogenesis.[9]

To summarize, the molecular mechanisms of oncogenesis of ATL, and in particular the mechanisms and role of selective oligoclonal proliferation, are incompletely understood. Here, in a large cohort of ATL patients and geographically matched asymptomatic HTLV-1 carriers, we used a quantitative high-throughput sequencing approach to test the hypothesis that the genomic environment flanking the proviral integration site is associated with malignant transformation of HTLV-1–infected clones and correlated the findings with both the clinical subtype of ATL and genetic and epigenetic modifications of the HTLV-1 provirus.

Methods

Study subjects and control cell lines

Blood or lymph node samples were donated by 221 ATL patients and 75 asymptomatic HTLV-1 carriers (ACs) from the Kumamoto region of Japan, and DNA was extracted at the Institute for Viral Research, Kyoto University, Japan, with written consent in accordance with regulations defined by the Japanese Government and Kyoto University. This study was conducted in accordance with the Declaration of Helsinki. This study was approved by the UK National Research Ethics Service (reference 09/H0606/106). The chromosomal distribution of integration sites in the present cohort was compared with the distribution in samples from 2 previously described studies: individuals with natural (nonmalignant) HTLV-1 infection from Kagoshima, southern Japan,[11,12] and cells infected with HTLV-1 in vitro.[6,13] The rodent cell line Tarl2, containing a single copy of HTLV-1, was used for quantification of PVL. ATL control cell lines T-43 (methylated) and T-48 (unmethylated) were used as methylation controls.[14]

PVL quantification

PVL was measured by quantitative polymerase chain reaction (PCR) of *tax* and *actin* genes using ABI Fast SYBR green as per the manufacturer's protocol (Applied Biosystems), using PCR primers as previously described[15] and assuming a single copy of *tax*[7] and 2 copies of *actin* per cell. Thermal cycling conditions were 95°C for 20 seconds and 40 cycles each of 95°C for 1 second followed by 60°C for 20 seconds. Standard curves were generated using serial dilutions of the cell line Tarl2, as previously described.[6,13]

Long-range PCR to identify defective proviruses

An internal control region at the 3′ end of the HTLV-1 genome was amplified for each ATL case, followed by a long-range PCR to identify defective proviruses based upon the length of the long-range PCR product as published by Tamiya et al.[16] DNA was amplified using KOD Hot Start DNA polymerase (Toyoba, Novagen). Primers for the control PCR and cycling conditions were 5′-CTCTCACAGTGGGCTCGAGA-3′ and 5′-CAAAGACGTAGAGTT GAGCAAGC-3′, 95°C for 2 minutes, 30 cycles: 95°C for 20 seconds, 59°C for 10 seconds, and 70°C for 48 seconds, followed by 70°C for 5 minutes. The primers and cycling conditions for the long-range PCR were 5′-CTTAGAGCCTCCCAGTGAAAAACATTTCC-3′ and 5′-GATG CATGGTCCTGCAAGGATAACA-3′, 95°C for 2 minutes, 30 cycles: 95°C for 20 seconds, and 66°C for 175 seconds, followed by 72°C for 15 minutes. The PCR products were electrophoresed on a 1% agarose gel with expected product size of 2.85 kb for the control PCR and 6.5 kb for a complete long-range product. A long-range product shorter than 6.5 kb defines a type 1 defective provirus; failure to amplify any long-range product identifies a type 2 defective provirus.[16]

Exon 2 and exon 3 tax gene sequencing

Tax protein is 353 amino acids in length: exon 2 provides the methionine start codon, and the remaining amino acids are derived from exon 3. Exons 2 and 3 were sequenced in ATL samples with a complete provirus. Exon 2 was amplified using PCR products from long-range PCR using Phusion high-fidelity DNA polymerase (New England Biolabs [NEB]). Primers and cycling conditions were 5′-CCTCAGCAATAAACAAACCC-3′ and 5′-CAATTG TGAGAGTACAGCAG-3′, 98°C for 30 seconds, 20 cycles: 98°C for 5 s seconds, 51.5°C for 20 s seconds, and 72°C for 10 seconds, followed by 72°C for 5 minutes. PCR products were inspected on 2% agarose gel for product length (318 bp). Exon 3 was amplified from the control long-range PCR product using Phusion high-fidelity DNA polymerase (NEB). Primers and cycling conditions were 5′- ATACAAAGTTAACCATGCTT-3′ and 5′-AGACGTCAGAGCCTTAGTCT-3′, 98°C for 30 seconds, 20 cycles: 98°C for 5 seconds, 51.5°C for 10 seconds, and 72°C for 22 seconds, followed by 72°C for 5 minutes. PCR products were inspected on a 2% agarose gel for product length (1120 bp) and sequenced by Sanger sequencing using 6 different sequencing primers to capture the entire exon (5′-ATACAAAGTTAACCA TGCTT-3′, 5′-CGTTATCGGCTCAGCTCTACA-3′, 5′-TTCCGTTCC ACTCAACCCTC-3′, 5′- AGACGTCAGAGCCTTAGTCT-3′, 5′-GGGTT CCATGTATCCATTTC-3′, and 5′- GTCCAAATAAGGCCTGGAGT-3′).

Methylation-specific PCR (MS-PCR)

MS-PCR was undertaken on ATL samples with a complete provirus but without a nonsense mutation of the *tax* gene. Takeda et al[17] showed that MS-PCR correlates with bisulfite sequencing PCR and with the methylation status of the promoter/enhancer Tax-response element-1 in the 5′ long terminal repeat (LTR). DNA was treated overnight with sodium bisulfite (Sigma) and purified using Zymo EZ Bisulfite DNA cleanup as per the manufacturer's protocol (Zymo Research). DNA was amplified by heminested PCR using JumpStart RedTaq polymerase (Sigma). Primers for the first PCR reaction for methylated DNA were 5′-TTAAGTCGTTTTTAGGCGTTGAC-3′, 5′-AAA AAAATTTAACCCATTACC-3′ and for unmethylated DNA 5′- TTAA GTTGTTTTTAGGTGTTGAT-3′, 5′-AAAAAAATTTAACCCATTACC-3′. The thermal conditions for first PCR were 94°C for 2 minutes, 35 cycles: 94°C for 30 seconds, 53°C for 30 seconds, and 72°C for 2 minutes. Primers for the hemi-nested methylated PCR were 5′-GAGGTCGTTATTTACGTCGGTT GAGTC-3′, 5′-AAAAAAATTTAACCCATTACC-3′ and unmethylated PCR primers 5′-GAGGTTGTTATTTATGTTGGTTGAGTT-3′, 5′-AAAAAAA TTTAACCCATTACC-3′. The cycling conditions for the second PCR were 94°C for 2 minutes, 30 cycles: 94°C for 30 seconds, 57°C for 30 seconds, and 72°C for 2 minutes, followed by 72°C for 5 minutes. The PCR product was inspected on a 2% agarose gel for length (428 bp). MS-PCR primers did not amplify unconverted HTLV-1 or host genomic DNA.

T-cell receptor (TCR) gene rearrangement studies

TCR-γ gene rearrangement studies were undertaken in the Imperial Molecular Pathology Laboratory, Hammersmith Hospital (London, United Kingdom) using the established BIOMED-2 protocol followed by heteroduplex analysis and/or GeneScanning. GeneScan analysis was performed on an ABI 3130 genetic analyzer using GeneMapper 4.0 (Life Technologies).

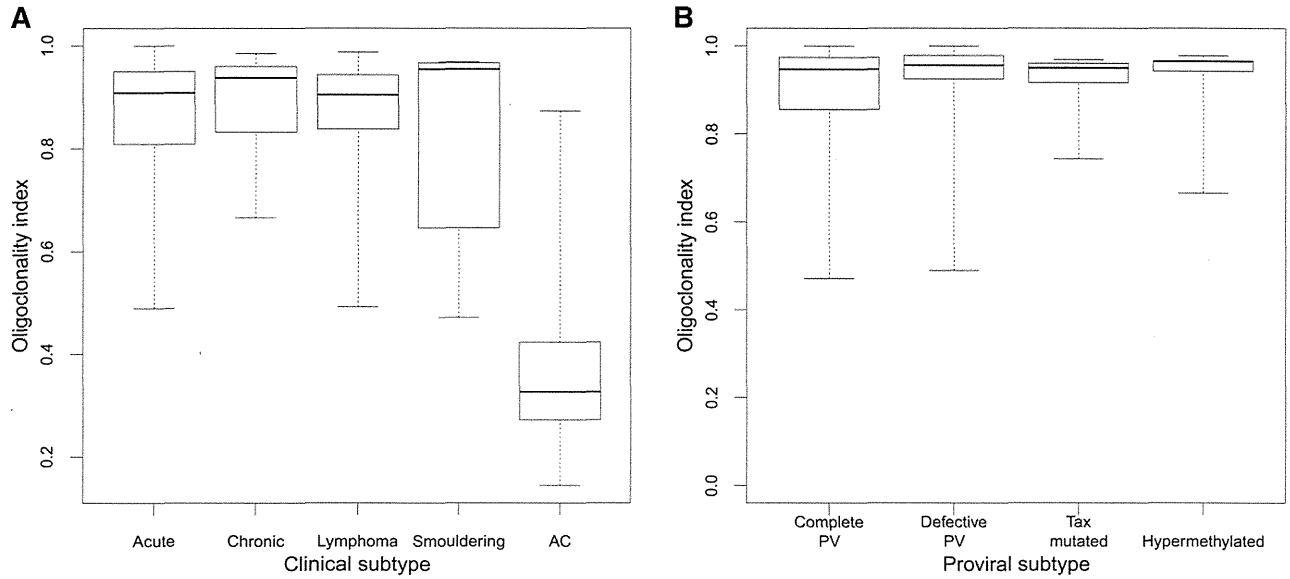

Figure 1. OCI by clinical and proviral subtype. (A) Median OCI of the ACs was 0.33 (range, 0.14-0.87), and median OCI for the ATL (all subtypes combined) was 0.91 (range, 0.47-1.0). There was no difference in OCI between ATL clinical subtypes. (B) There was no difference in OCI between the different mechanisms of proviral silencing. PV, provirus.

Integration site mapping and quantification

The high-throughput protocol for identification and quantification of proviral integration sites was carried out as previously described.[6] Mapped integration sites were compared with a set of randomly generated in silico genomic sites (n = 175 505) as previously reported.[13]

Bioinformatic annotation of genomic environment

Transcription units and cytosine guanine dinucleotide island data were retrieved from the National Center for Biotechnology Information (ftp.ncbi.nih.gov/gene/) and University of California, Santa Cruz tables, respectively. Epigenetic marks were annotated according to primary $CD4^+$ T-cell chromatin immunoprecipitation sequencing data published by Barski et al.[18] Transcription factor binding sites were obtained from published data sets (supplemental Figure 1 available at the *Blood* Web site) from chromatin immunoprecipitation sequencing experiments on primary human $CD4^+$ T cells or other primary human cells or cell lines, as previously described.[13] Cancer-associated gene data sets are defined by Sadelain et al.[19] Annotated genomic positions were compared with the integration site data using the hiAnnotator R package kindly provided by N. Malani and F. Bushman (University of Pennsylvania; http://malnirav.github.com/hiAnnotator).

Diversity estimator

The diversity estimator (DivE)[20] was used to estimate the total number of clones in addition to those observed. DivE involves fitting many mathematical models to nested subsamples of individual-based rarefaction curves. Estimates from the best-performing models are aggregated to produce the final estimate.[20] DivE requires an estimate of the number of cells in the blood; because the absolute PBMC count for each case was unknown, DivE estimates were calculated for each patient over 2 orders of magnitude of variation in the PBMC count (3×10^9/L, 50×10^9/L, and 500×10^9/L).

Statistical analysis

Statistical analysis was carried out using R version 2.15.2 (http://www.R-project.org/). The oligoclonality index (OCI; Gini coefficient)[6,21] was calculated using the R reldist package[22] (http://CRAN.R-project.org/package=reldist). Two-tailed nonparametric tests (Mann Whitney *U*, Fisher's exact, χ^2) were used for all comparisons. Bonferroni's correction for multiple testing was applied where appropriate. To test the hypothesis that 2 observed HTLV-1 integration sites were present in 1 T-cell clone, we used the Gaussian approximation to the binomial distribution (supplemental Figure 3). To identify clusters of integration sites or genomic hotspots of integration, we used R software developed by Presson et al[23] (http://www.biomedcentral.com/1471-2105/12/367). Functional categories of genes were analyzed through the use of Ingenuity Pathway Analysis (Ingenuity Systems; http://www.ingenuity.com).

Results

The ATL samples are derived from a representative cohort

We analyzed 197 cases of ATL; patients' characteristics are detailed in supplemental Figure 4. Systematic analysis of the proviral structure showed a complete provirus in 46% of cases, putatively capable of Tax expression; 39% of cases contained a defective provirus, 7% contained a nonsense mutation of the *tax* gene, and 8% contained a hypermethylated promoter in the 5′ LTR. There was no significant difference in OCI between ATL clinical subtypes (median OCI = 0.91) or by proviral subtype (median OCI = 0.91); the median OCI in asymptomatic carriers was 0.33, in the range previously reported[6] (Figure 1).

The median absolute number of $HTLV\text{-}1^+$ T-cell clones (estimated by the DivE technique) in the circulation in ACs was 9054. The median number of clones in the ATL cases was 1741 (assuming PBMC = 3×10^9/L) or 2154 (assuming PBMC = 50×10^9/L). These results show that although the white cell count may vary over an order of magnitude between individuals with ATL, the estimated number of distinct clones underlying the malignant clone remains relatively stable (~2000).

In 91% of ATL cases, a single copy of HTLV-1 is integrated into the host genome

In our protocol, the quasi-random DNA shearing by sonication allows unbiased, quantitative detection of proviruses[6,24] and therefore

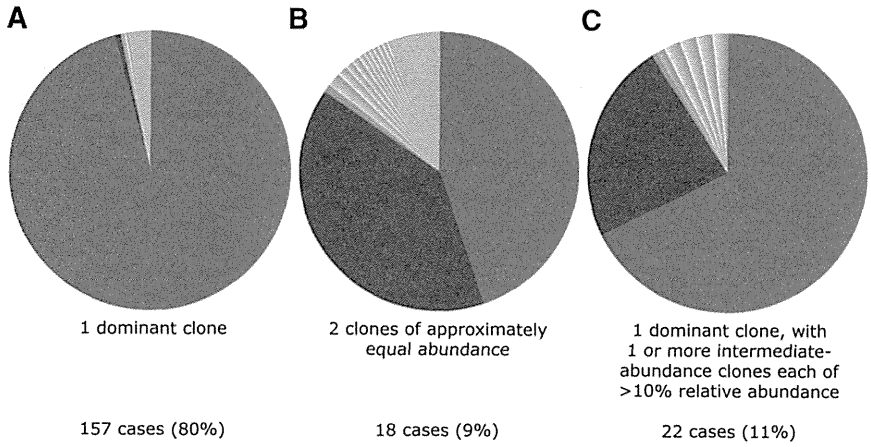

Figure 2. Examples of 3 typical clonal structures of ATL cases. Each sector in the pie charts depicts the relative abundance of the respective integration site. (A) Typical "monoclonal" ATL tumor sample; PVL = 63% (relative abundance of dominant clone = 97% of PVL). (B) Two equally abundant integration sites (relative abundance respectively 44% and 39% of PVL); PVL = 9%. (C) ATL with dominant clone and additional intermediate-abundance clone (relative abundance respectively 67% and 23% of PVL); PVL = 241%.

enabled us to quantify the presence of 2 abundant integration sites in an ATL tumor (Figure 2). In 157 out of 197 samples (80%), as expected, a single dominant proviral integration site was observed, with a median relative abundance of 99.4% of the PVL (range, 35% to 100%). However, in 40 out of 197 samples (20%), the presence of only a single provirus was less certain, because >1 abundant integration site was observed. In each of these 40 cases, there was 1 "large" ATL integration site with relative abundance >35% and an additional site with a relative abundance >10%. The question arises whether these represented 2 proviruses in 1 malignant clone or if there were 2 distinct abnormally expanded clones. If a single malignant clone contains 2 proviruses, then each will be present at the same frequency, assuming a steady kinetic state and no recent reinfection with a second provirus, and the clone will carry a single TCR gene rearrangement. Alternatively, if there are 2 large independent clones, then the 2 integration sites will differ in abundance and 2 distinct TCR gene rearrangements will be detected. We found no significant difference in the abundance of 2 integration sites in 18 cases (9.1% of cohort) (supplemental Figure 3), suggesting the presence of 2 proviruses in a single tumor clone. In 22 cases (11% of the cohort), we observed a large ATL clone and a second clone of abnormal but significantly lower abundance. TCR-γ gene rearrangement analysis of these 40 samples confirmed a monoclonal population in 7 out of 40 cases (3.1%); this technique may underestimate monoclonality, owing to the possibility of a second rearranged TCR-γ allele. To conclude, a single dominant provirus was detected in 91% of cases, whereas in 9% of tumors there was evidence of 2 proviruses. These results are consistent with the finding of multiple proviruses in 11% of cases reported by Tamiya et al[16] using low-throughput techniques.

Binning of clones into small, intermediate, or large

In subsequent analysis, each clone was binned according to its relative abundance, ie, the proportion of the subject's PVL occupied by that clone. Each ATL case contained at least 1 abundant clone with a relative abundance >35% (n = 217 clones) that was defined as large; "small" clones were defined as those of relative abundance <1% (n = 5925), and such clones constitute the great bulk of PVL in nonmalignant HTLV-1 infection.[6,13] Clones (n = 90) that constituted between 1% and 35% of PVL were classified as intermediate abundance. Clones (n = 16 909) identified in the AC cohort were analyzed together, because only 4 of these clones fulfilled the large-clone classification (supplemental Figure 2).

Large ATL clones have the same genomic characteristics as small (nonmalignant) clones, whereas intermediate-sized clones have unique genomic characteristics

The intermediate-abundance clones observed in 24% of cases (48/197) in addition to the large (presumed malignant) clone were larger (ie, had a greater absolute abundance) than any clones previously observed in AC or HAM/tropical spastic paraparesis cohorts.[6,13] Because progressive oligoclonal proliferation has been postulated to precede malignant transformation, we tested the hypothesis that there is a stepwise progression in the frequency of integration site characteristics from low-abundance clones through intermediate-abundance to large ATL clones. The results showed that the large, presumed malignant ATL clones had integration site characteristics indistinguishable from those of the low-abundance clones present in ACs and in patients with ATL. In contrast, the integration sites present in the intermediate-abundance clones in ATL patients, which are not observed in nonmalignant infection, differed from both the low- and high-abundance clones in each genomic attribute examined (Figure 3). Specifically, the intermediate-abundance clones lacked the associations observed in the ACs and in the low-abundance and high-abundance clones seen in ATL, with either transcriptional orientation or proximity to transcription start sites, cytosine guanine dinucleotide islands, or activatory epigenetic marks. Instead, the intermediate-abundance clones showed an association with proximity to inhibitory epigenetic marks (Figure 3C) and specific transcription-factor binding sites (TFBSs) within 100 bp upstream or downstream of the integration site, notably binding sites for P300/CBP-associated factor (odds ratio [OR] = 4.78), Rad 21 (part of the cohesin complex) (OR = 4.08), and ZNF263 (OR = 5.57). These effects disappeared at 1 kb from the integration site (Figure 3A). Integration in proximity to these specific TFBSs was identified in 8 out of 197 tumor samples (4.1% of cohort).

There are no hotspots of integration associated with large ATL clones

All data sets were further annotated to investigate the proximity of the integrated provirus to the nearest cancer-associated gene. The frequency of integration was significantly higher than random expectation within 10 kb of oncogenes in clones from ACs and low-abundance clones from ATL patients, and within 150 kb in the large ATL clones; this association was not observed in the intermediate-abundance clones. We conclude that integration in proximity to these cancer-related genes confers a survival advantage

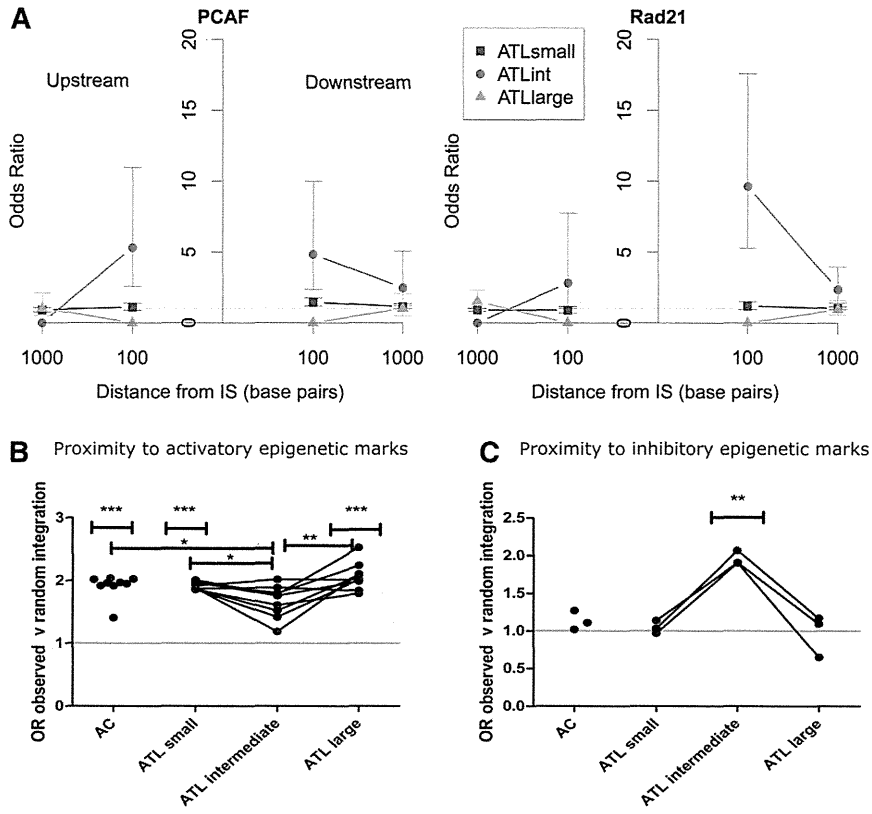

Figure 3. Intermediate-abundance clones in ATL cases contained proviruses with distinct genomic marks. (A) The OR of integration in proximity to specific TFBSs compared with AC is illustrated for 2 TFBSs, P300/CBP-associated factor binding sites (PCAFbsites) and Rad21. (See supplemental Figure 1 for full list of TFBSs tested). The y-axis shows the OR compared with ACs. The x-axis shows the distance in base pairs (logarithmic scale) from the integration site upstream (left-hand side) or downstream (right-hand side). "Upstream" and "downstream" are defined with respect to the sense strand of the HTLV-1 provirus. The junction of the x-axis and y-axis represents the integration site. There were no independent TFBS predictors for small clones (blue squares) or large clones (green triangles) in ATL cases compared with ACs (OR = 1) or when compared with each other or to random data sets (not illustrated). Independent TFBSs associated with intermediate-abundance clones in ATL cases (red circles) (PCAFbsites, Rad21) at 100 bp upstream or downstream compared with ACs are illustrated. (B) OR of integration in proximity to activatory epigenetic marks compared with random sites. AC, small, and large clones in ATL cases showed a significant bias toward integration in proximity to activatory epigenetic marks. There was no such bias in the intermediate-abundance clones. (C) OR of integration in proximity to inhibitory epigenetic marks compared with random. AC, small, and large clones in ATL cases showed no bias toward integration in proximity to inhibitory marks compared with random sites, whereas intermediate-abundance clones showed a bias toward inhibitory epigenetic marks (see supplemental Figure 1 for details of epigenetic marks tested). IS, integration site.

in vivo but does not play a significant role in leukemogenesis per se. The use of the powerful bioinformatic method of Presson et al[23] confirmed that there were no significant hotspots of integration associated with ATL.

The ontology of the nearest downstream gene was associated with the malignant clone in 6% of ATL cases

As a further test of the hypothesis that HTLV-1 proviral integration near host genes in a certain functional category confers a proliferative advantage on the infected T-cell clone, we used Ingenuity Pathway Analysis software to analyze the ontology of the nearest host genes upstream and downstream of each integration site. The results showed a significant overrepresentation of genes in 3 cellular pathways ("cell morphology," "immune cell trafficking," and "hematological system development and function") in the large ATL ("malignant") clones, but not in either the low- or intermediate-abundance clones (Figure 4). The 11 genes responsible for this significant association (*CD46*, *ITGA4*, *DPYSL2*, *RAP2A*, *CASP8*, *CDKN2A*, *GTF2I*, *TACR1*, *BCL2*, *IL6ST*, and *HGF*) accounted for 11 ATL cases (5.8% of the cohort) of different clinical subtypes. Furthermore, these effects were only seen in the nearest host gene downstream, regardless of its transcriptional orientation relative to the provirus. The median distance from the integration site to these nearest genes was 13.7 kb (range, 0.6-294 kb) compared with a median distance of 122.3 kb from all integration sites to the nearest cancer-associated gene (P = .009, Mann Whitney U test).

The HTLV-1 provirus preferentially survives in acrocentric chromosomes in vivo

Meekings et al[25] reported that the frequency of HTLV-1 proviruses in chromosome 13 was significantly higher in vivo than expected by chance, but the biological significance of this observation was uncertain. Here, using our quantitative, high-throughput technique, we observed a significant excess of integrations in chromosomes 13, 14, 15, and 21 compared with random and in vitro data sets. This excess was seen in all infected individuals and was not confined to those with ATL. There was a trend toward excess integrations in chromosome 22, but this was not statistically significant (Figure 5). These findings were validated with a second cohort of independent AC samples from the Kagoshima region of Japan. The chromosomal distribution of proviruses in the intermediate-abundance and large ATL clones was not significantly different from random, perhaps because of the small number of clones (n = 307).

Discussion

Oligoclonal proliferation of HTLV-1–infected T-cells is a cardinal feature of HTLV-1 infection. It has long been believed that this oligoclonal proliferation is primarily responsible for maintaining the high PVL of HTLV-1, which is the strongest correlate of risk of both the inflammatory (HAM) and malignant (ATL) diseases. However, we recently showed that the PVL correlates with the total number of infected clones, but not with the degree of oligoclonal proliferation as measured by the OCI.[6,13] Here, we show that ATL is frequently accompanied by a population of abnormally abundant HTLV-1–infected T-cell clones underlying the largest, putatively malignant clone. This observation suggested that such intermediate-abundance clones might represent an intermediate stage of malignant transformation between the low-abundance clones and the fully transformed, largest clone. However, we found that the host genomic attributes of the integration site in the large ATL clones closely

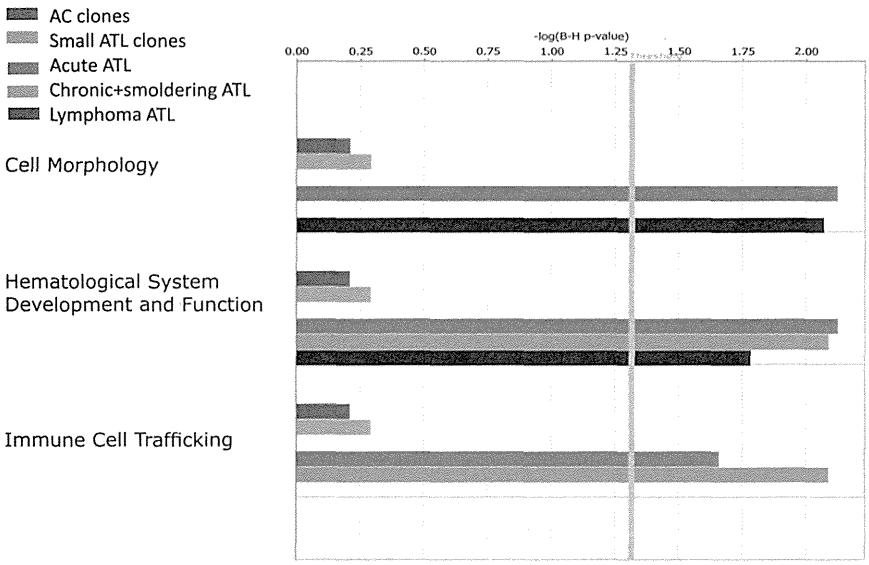

Figure 4. Functional classification of gene ontologies overrepresented among the large ATL clones. Functional categories significantly overrepresented among the random, AC, ATL small, intermediate, and large ATL clones as analyzed by Ingenuity software using the Ingenuity Pathways Knowledge Base (IPKB) gene population as baseline. Horizontal bars are only visible where there was a statistical overrepresentation of the pathway compared with the IPKB. Because there were no overrepresented pathways involving the random integration sites or intermediate-abundance clones in ATL cases, the bars are not visible. The vertical yellow threshold represents the line of statistical significance ($P < .05$) after correction (Benjamini-Hochberg) for multiple testing. The numbers of searchable genes for comparison with the IPKB were random (n = 96 706), AC (n = 5679), ATL small (n = 1628), ATL intermediate (n = 87), or ATL large (acute n = 141, lymphoma n = 31, chronic and smoldering n = 38).

resembled those of the low-abundance clones present both in ATL patients and in those with nonmalignant infection, whereas the integration site characteristics of the intermediate-abundance clones differed from both the low- and high-abundance clones and from the clones observed in nonmalignant cases of HTLV-1 infection. We conclude that the malignant clone does not arise from the intermediate-abundance clones but instead from the low-abundance clones. This conclusion is consistent with the observations that the low-abundance clones constitute the bulk of the PVL in HTLV-1 infection[6] and that the risk of ATL is correlated with the PVL.[2,4] We have also observed cases in which the malignant clone emerges from the large population of low-abundance clones, not from the preexisting oligoclonally expanded population.[26] Finally, this conclusion is also consistent with our recent observation[27] of highly oligoclonal proliferation and a small total number of clones in human T-lymphotropic virus type 2 infection, which does not cause malignant disease.

We therefore propose that the major determinant of the risk of ATL is the absolute number of clones: the larger the number, the greater the chance of malignant transformation. It is likely that the number of HTLV-1–infected clones present in an individual during chronic infection is determined chiefly by the efficiency of the host's CTL response to the virus, which in turn is determined by the HLA and killer immunoglobulin-like receptor genotype.[10,28]

The observation that the abnormally expanded intermediate-abundance clones seen in patients with ATL do not share genomic characteristics with either the polyclonal background or the malignant clones suggests that the intermediate-abundance clones arise as a consequence of ATL development and are not causative. One possibility is that these clones survive and proliferate as a consequence of the severely impaired immune response in ATL. The malignant clones in ATL use well-described mechanisms to silence Tax, either before or after malignant transformation, which allows them to escape the immunodominant CTL response and so confers a survival advantage. Once the malignant clone has emerged, the resulting immune impairment may allow the intermediate-abundance clones to survive despite continued expression of viral genes.

As expected, we did not identify any hotspots of integration, although analysis of the ontology of flanking genes demonstrated a functional overrepresentation of certain genes that are known to be dysregulated in many leukemias. This effect was significant only in the large (presumed malignant) ATL clones and only when considering the ontology of the nearest host gene downstream; there was no effect of the upstream host gene. Further, these specific genes lay very close (median 13.7 kb) to the provirus, suggesting a mechanistic interaction between the provirus and the downstream gene. Although the associations reported here between ATL and individual genes and genomic features account for a small proportion of the observed cases of ATL, these results indicate that transcriptional interactions between the provirus and the flanking host genome influence the risk of malignant transformation. Vogelstein recently estimated that each tumor-driver mutation contributes a survival advantage of ~0.4% to

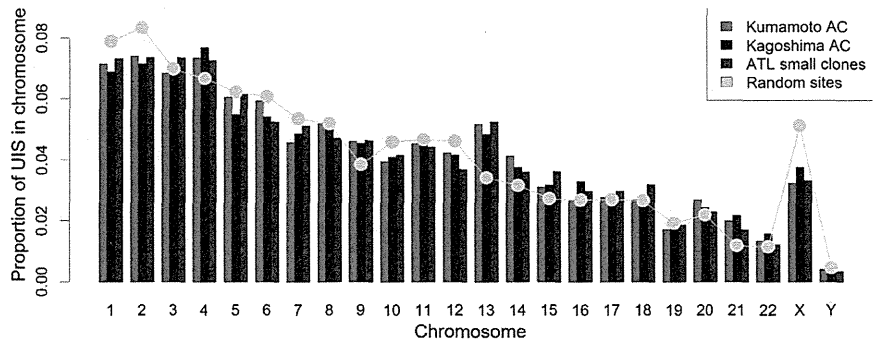

Figure 5. Preferential survival of HTLV-1 in vivo in chromosomes 13, 14, 15, and 21. The proportion of unique integration sites (UIS) per chromosome is shown for 2 independent AC data sets (Kumamoto and Kagoshima) and the small clones in ATL cases. The yellow line shows the frequency of sites in the random data set. There were an increased number of integrations in chromosomes 13, 14, 15, and 21 in the clones of asymptomatic carriers and small clones in ATL cases compared with random. The bias remained in chromosomes 13 and 15 when compared with a previously reported data set[6] of integration sites from Jurkat cells infected in vitro with HTLV-1.